gear TECHNOLOGY®

JUNE 2026

Gearbox Repair
CTI Symposium
Metrology
and more

TECHNICAL

Analytical Calculation of the Gear Body Stiffness of Face Gears

geartechnology.com

Gear Technology is POWERED by the MOTION + POWER MANUFACTURERS ALLIANCE™

GEAR CUTTING SOLUTIONS

CONTENTS

gear TECHNOLOGY®

JUNE 2026

feature

22

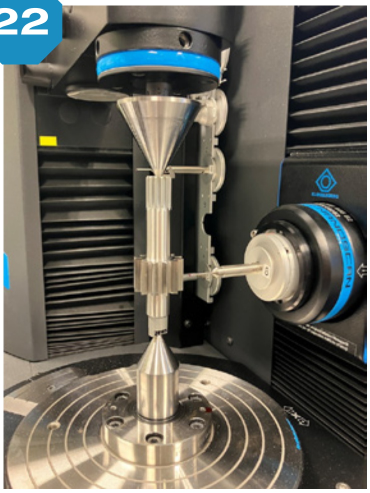

technical

41

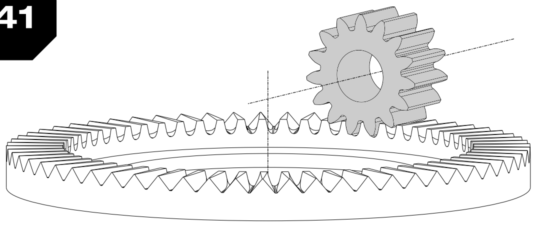

Vol.43. No.4 GEAR TECHNOLOGY. The Journal of Gear Manufacturing (ISSN 0743-6858) is published monthly, except in February, April, October and December by The Motion + Power Manufacturers Alliance, 1001 N Fairfax Street, Suite 500, Alexandria, VA 22314, (847) 437-6604. Periodical postage paid at Arlington Heights, IL, and at additional mailing office (USPS No.749-290). The Motion + Power Manufacturers Alliance makes every effort to ensure that the processes described in GEAR TECHNOLOGY conform to sound engineering practice. Neither the authors nor the publisher can be held responsible for injuries sustained while following the procedures described. Postmaster: Send address changes to GEAR TECHNOLOGY. The Journal of Gear Manufacturing. 1001 N Fairfax Street, Suite 500, Alexandria, VA 22314.

gear TECHNOLOGY®

Vol. 43. No. 4

Zeiss and Bosch compare conventional touch measurement with optical fringe projection on p. 22.

gear TECHNOLOGY®

GT REVOLUTIONS

A Conference Worth Crossing the Atlantic For

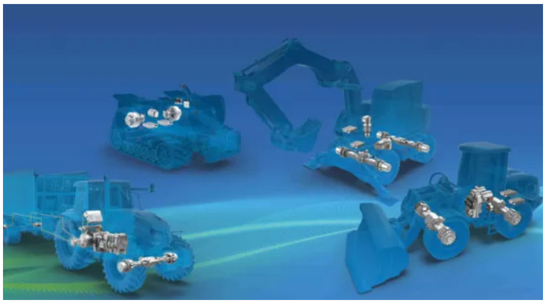

I went to the VDI International Conference on Gears in Garching in 2023. As an editor for *Gear Technology*, what stuck with me was not any single presentation per se, but how few Americans were there. AGMA was listed as an associated organization. Ahmet Kahraman from Ohio State sat on the program committee. There were American names on the schedule. But the actual turnout from our side was thin. The Europeans filled the place. So did the Japanese, the Chinese, the Koreans. It left me convinced that American engineers have a lot to gain from and contribute to these conversations.

geartechnology.com/a-conference-worth-crossing-the-atlantic-for

EMAG Examines Requirements for Rotor Shafts for Electric Drives

With the rise of electric mobility, the focus in manufacturing is shifting significantly: Components that could "run along" in internal combustion engines due to masking noises and vibrations are evaluated much more critically in electric drives. The reason is simple: The internal combustion engine generates a broad spectrum of noise that masks many background sounds. In electric drives, this acoustic "background noise" is largely absent, making deviations in shape, position, and surface significantly more noticeable.

geartechnology.com/emag-examines-requirements-for-rotor-shafts-for-electric-drives

GT VIDEOS

Liebherr Hobbing Machine LC 280 DC with FlexChamfer

The LC 280 DC gear hobbing machine from Liebherr is designed for precise gear cutting up to module 4.5 mm. It combines high productivity with advanced technology, featuring simultaneous FlexChamfer for efficient deburring and chamfering during the hobbing process.

geartechnology.com/videos/liebherr-hobbing-machine-lc-280-dc-with-flexchamfer

MPMA Media
1001 N. Fairfax Street 5th Floor
Alexandria, VA 22314
Phone: 847-437-6604 | Fax: 847-437-6618

EDITORIAL

Director, Editorial Content
Matthew Jaster
jaster@motionpower.org

Senior Editor
Aaron Fagan
fagan@motionpower.org

Associate Editor
Jennifer Jensen
jensen@motionpower.org

Technical Editors
John Lange. Joseph Mihelick. Charles D. Schultz. P.E.. Mike Tennutti. Frank Uherek

GRAPHIC DESIGN

Design Manager
Jess Oglesby
oglesby@motionpower.org

ADVERTISING

Manager, Member Engagement and Sales
Katie Mulqueen
mulqueen@motionpower.org

Media Fulfillment & Member Services Coordinator
Baillie Bodle
bodle@motionpower.org

CIRCULATION

Circulation Manager
Jessica Schuh
schuh@motionpower.org

MANAGEMENT

President
Jenny Blackford
blackford@motionpower.org

FOUNDER

Michael Goldstein founded *Gear Technology* in 1984 and served as Publisher and Editor-in-Chief from 1984 through 2019. Thanks to his efforts, *the Michael Goldstein Gear Technology Library,* the largest collection of gear knowledge available anywhere, will remain a free and open resource for the gear industry. More than 40 years' worth of technical articles can be found online at *geartechnology.com.* Michael continues working with the magazine in a consulting role and can be reached via e-mail at *mwg42@hotmail.com.*

THE GEAR INDUSTRY'S INFORMATION SOURCE

GEAR UP!
Military grade reliability
in the air and on the ground.
FOREST CITY GEAR
Seventy Years of Gears!
AGMA | ISO 9001 | AS9100 | ISO 13485 | ITAR Certified
forestcitygear.com
Copyright ©2025 Forest City Gear. All Rights Reserved.

Know the Place for the First Time

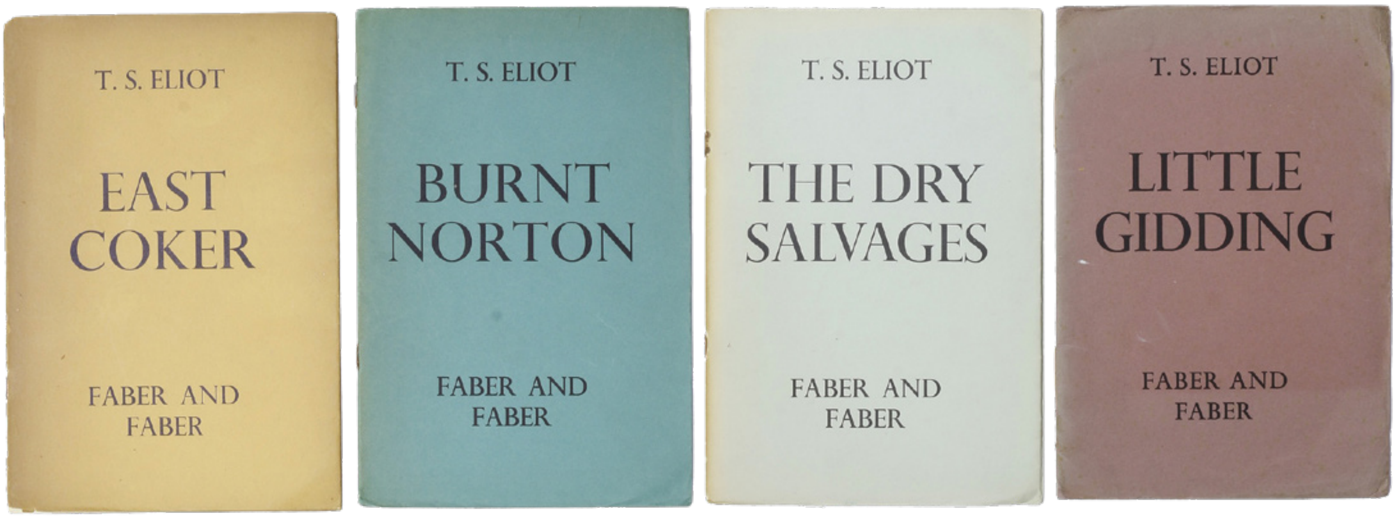

The original Faber and Faber pamphlet editions of T.S. Eliot's Four Quartets: East Coker (1940), Burnt Norton (1941), The Dry Salvages (1941), and Little Gidding (1942). The quartets were published individually before being collected into a single volume in 1943.

Aaron Fagan, Senior Editor

I've been reading T.S. Eliot's *Four Quartets* for most of my adult life. My relationship to it has evolved the way great long friendships do. There are years I stay in touch and years I drift away. When I come back, the poem hasn't changed, but I have. Different passages come in and out of focus depending on where I am in my life and the day I am reading. A line near the end of "Little Gidding," the last of the quartets, summarizes this sustained experience of the poem itself: *We shall not cease from exploration / And the end of all our exploring / Will be to arrive where we started / And know the place for the first time.*

In the beginning, I read that—limited to an intellectual understanding—as a statement about the nature of wisdom, but now I understand it otherwise, more in practical terms. It's about the difference between looking at something and looking at something and actually seeing it. You can experience something for years, and then a shift in method or attention or necessity makes the whole thing legible in a way it wasn't before.

I recently had the good fortune to drive down to Lufkin, TX, and spend a morning with Scott Franks at Luftex. Part of the article that came out of that discussion tells a story about a steel plant with a recurring gear failure that nobody could diagnose. While the gears rated fine and the housing checked out, everything that should have explained the problem didn't. What he eventually found had been sitting in plain sight the whole time, and once you hear it, you'll wonder how anyone missed it. See p. 18 to hear him tell it.

Groß and Schmidt (p. 22) aimed three different measuring systems at the same tooth flank and discovered that what you see depends, both literally and figuratively, on how you look. The tactile instruments and the optical fringe projector agreed in some places and disagreed in others. The same surface reveals different information. It's not that one system was wrong. Each one was seeing a version of the truth shaped by its own physics.

Berger (p. 41) went back to a gear body stiffness method that's been in use since 1953, a formulation so established it lives inside ISO standards, and found that it produces the wrong trend when applied to face gears. There was nothing wrong with the math. It was designed for cylindrical gears, not to describe a face gear. He swapped the geometric model, and the answer reversed.

Even the CTI Symposium coverage (p. 20) reads this way. Micky Bly from Stellantis came back from visiting automotive plants in Asia and told a room full of powertrain engineers that the competition isn't what they thought it was. The threat was there before Bly went to look at it. He just went and looked.

I don't have a grand theory about any of this. But the people in these pages share a common bond: nobody found something that wasn't there before; they went back to something familiar and finally saw what it had been trying to show them.

MOTION + POWER
MANUFACTURERS ALLIANCE™

Growing the Next Generation

Steve Janke, Chair, MPMA Board of Directors

When I was first invited to join what would become the Strategic Networking Leadership Forum (SNL)—then in its earliest meetings as the Future Leaders Council—I wasn't sure exactly what to expect. I was a relatively new face in the association, still finding my footing in a room full of other young owners and executives, eager to learn from each other. But I showed up, and that decision changed the trajectory of my involvement with this organization in ways I couldn't have anticipated.

I joined what I recall was the second or third meeting of the group, as the founders were still working to get it off the ground. From the beginning, the energy was different. This wasn't a committee focused on policy or procedure. It was a group of next-generation leaders—gear shop owners, executives, rising managers—who genuinely wanted to learn from one another and invest in the future of the industry. I was immediately drawn in.

What stood out most to me, and what I still think about today, were the facility tours. There is something uniquely valuable about walking the floor of a peer's operation. You see how they've solved problems you're wrestling with. You notice equipment choices, workflow decisions, quality processes—things you'd never learn from a trade publication or a conference panel. Those tours sparked some of the most honest and productive conversations I've had in my career. They created a level of trust among participants that is rare in any industry, let alone one as specialized and competitive as ours.

The relationships I built through the SNL were equally formative. Getting to know other gear shop owners and CEOs on a personal level—understanding their challenges, their philosophies, their ambitions—gave me a broader perspective on our industry that I carry with me to this day. It also gave me the confidence to take on greater responsibility within the association. My involvement with the SNL eventually led me to chair the Trade Show Committee, and that experience set me on the path to where I stand today.

The Future Leaders Council and the SNL produced four Chairmen of this association. I am the last of them. That fact fills me with both pride and a sense of urgency, because we need to refill that pipeline. My business would not be where it is today if I hadn't gotten involved with this alliance.

As I step into the role of Chairman of the Board for the Motion Power Manufacturers Alliance, one of my primary commitments is to help identify and develop the next generation of leaders for this organization. We need to find those people now, bring them into the work of the association, give them real responsibility, and invest in their growth. That doesn't happen by accident. It has to be intentional.

The other challenge I intend to take head-on is helping our membership navigate the rise of artificial intelligence. Larger companies have resources dedicated to this already. But I believe the greatest opportunity belongs to our smaller members—the agile, entrepreneurial shops that can adopt new tools quickly and use them to compete in ways that simply weren't possible a few years ago. The MPMA should be a resource and a catalyst for that conversation.

This industry has given me a great deal. The Future Leaders Council gave me a community when I was new, and a foundation when I was ready to lead. My goal as Chairman is to make sure the next generation has the same opportunity.

motionpower.org

Steve Janke
Chair, MPMA Board

Index

DEMONSTRATES STRATEGIES FOR COMPLETING EVERY JOB FASTER AT IMTS 2026

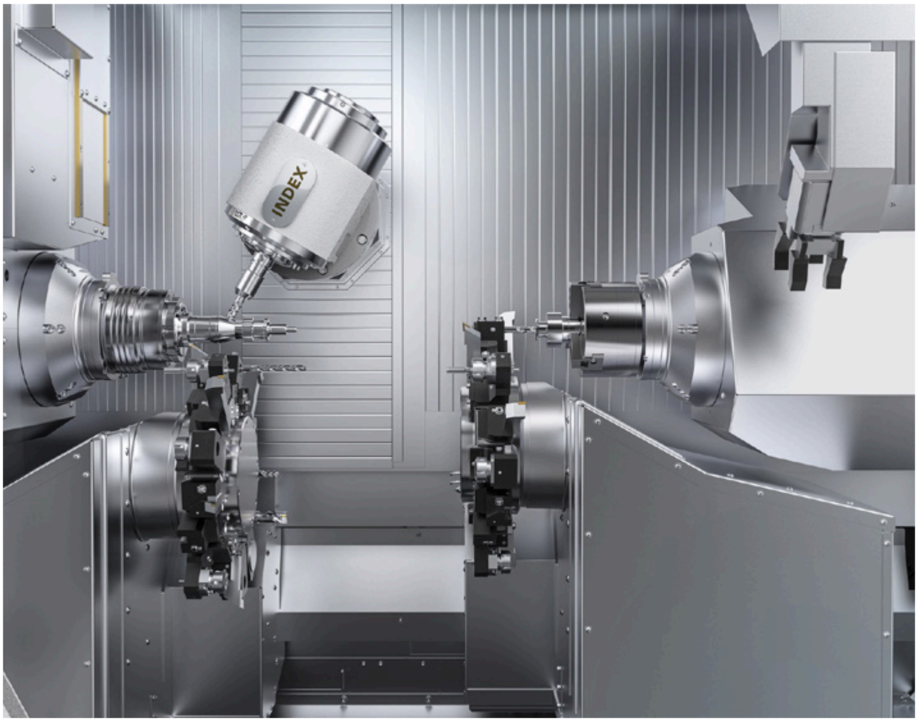

Index Corp. will present manufacturers with a variety of strategies to streamline production at IMTS 2026. Visitors to the company's Booth #339119 in the South Building will witness the North American debut of multiple new machines, including an entirely new design concept tailored to small part production. The company will also demonstrate its full portfolio of proven advanced machine technologies, as well as provide insight into how manufacturers can produce every job faster to maximize profitability.

"When we say every job faster, we are talking about the comprehensive perspective that manufacturers need to embrace to ship good parts as quickly as possible," Index President and CEO Michael Huggett said. "Cycle time reduction is a vital part of that, but it alone can't get a company to maximum profitability. With the technologies and experts we're bringing to IMTS, we're asking attendees to tell us about the parts they need to produce, then demonstrating how they can achieve the mix of cycle time, quality, reliability and automation needed to get the best possible result."

At the show, the Traub MS12-4 CNC multispindle will stand out as an entirely new machine concept making its North American debut. The machine effectively combines four Traub TNL12 single-spindle sliding headstock lathes into one machine with four primary spindles, four tool turrets, two or four counter spindles and up to four Flex-WT flexible tool carriers. A flexible, modular design enables the MS12-4 to be optimized for a manufacturer's specific production needs.

The MS12-4 brings the low cycle times and reliably precise performance of CNC multispindles to applications that are poor candidates for a drum-style multispindle. Because the stations of the MS12-4 concurrently produce fully finished parts, the machine allows optimization of a broader variety of components. Additionally, the inclusion of sliding headstocks for each of the machine's spindles allows the productivity of a multispindle to be achieved for long, thin parts, such as bone screws and small electrical components.

The Index G160 5-axis turn mill will also be demonstrated for the first time in North America. Built on a rigid, vibration-damping machine bed, the G160 incorporates a pair of highly dynamic direct-drive spindles, available with bar clearances of 1.64 in. (42 mm) or 2.56 in. (65 mm). An upper tool carrier with a B axis and direct-drive milling spindle enables full 5-axis machining while two lower tool turrets are capable of serving either of the machine's spindles. Manufacturers not requiring robust 5-axis capabilities can optionally select to replace the milling spindle with an upper tool turret. The machine is easily integrated with a variety of automation solutions and offers an assortment of options. Together, these features allow the G160 to be optimized for a diverse range of small, complex parts across all industry segments.

Visitors to Index's booth will have the opportunity to see its C200 production turning center from a new perspective. The machine will be on display with a plexiglass rear panel to provide visibility into its unique kinematics. Specifically, the C200 incorporates the Index SingleSlide system, which provides two degrees of movement in a single plane. This proprietary design enables high dynamic response while achieving exceptional vibration damping, resulting in shorter cycle times, excellent part quality and up to 30 percent increases to tool life.

Index will also be showcasing the MS24-8, the latest evolution of the company's family of drum-style CNC multispindles. With W-serration toolholders for quick setups and changeovers, eight main spindles and up to two swiveling synchronous spindles, the machine remains the fastest, most reliable means of production for a wide swath of small parts.

At the other end of the size spectrum, the G320 CNC turn mill for large parts will be on display. The G320 will be the largest of the family that Index has brought to IMTS, accommodating turning lengths up to 55.1 in. (1,400 mm) and diameters up to 9.8 in. (250 mm). Featuring high thermal and mechanical stability, high tool capacity and full 5-axis machining capabilities, the machine offers exceptional performance for large, complex workpieces with demanding quality requirements.

Additionally, Index will also demonstrate its Traub TNL20 turning center, which can quickly and easily changeover between sliding-headstock and fixed-headstock operation. The TNL20 is available in three distinct variations. The standard TNL20-9 provides simultaneous and precise machining with up to three tools. The TNL20-9B incorporates a B axis to enable the machining of highly complex part geometries. The TNL20-11 provides an additional front working attachment that enables simultaneous machining with up to four tools for even higher productivity.

Visitors to the Index booth will also learn about the latest additions to the company's iXworld cloud-based platform, which includes the iX4.0 productivity apps, iXservice portal and iXshop procurement portal. One Click Metal, a subsidiary of Index specializing in safe, affordable and easy-to-use 3D printing systems, will be in the booth as well. Representatives from Horn USA will also be on hand to discuss tooling provided for cutting demonstrations within the booth.

index-group.com/en_us/

Rego-Fix

RACES INTO IMTS WITH PRECISION TOOLHOLDING TECHNOLOGY

Rego-Fix USA will showcase its advanced toolholding solutions for manufacturers seeking enhanced precision, repeatability and reliability in their machining processes at IMTS 2026 in Booth #431822. The company will feature the original ER collet and its patented powRgrip toolholding system. Also on display will be an Ed Carpenter Racing (ECR) racecar, symbolic of Rego-Fix's ongoing sponsorship for the upcoming 2026 NTT IndyCar Series racing season.

Rego-Fix toolholding systems provide Swiss-precision machining for all manufacturing sectors, including motorsports, aerospace, automotive and medical, through engineered solutions that deliver accuracy, rigidity and repeatability in high-pressure environments that demand tight tolerances.

Developed in Tenniken, Switzerland, by Rego-Fix, the original ER collet is engineered for exceptional precision, versatility and reliability across a wide range of machining applications. Rego-Fix ER collets provide high-clamping force and superior concentricity for extending tool life while ensuring consistent part accuracy. The ER collet is available in multiple sizes and configurations to accommodate a broad clamping range, allowing shops to reduce tooling inventory without sacrificing performance. The ER collet remains the most widely used clamping unit in the world.

The Rego-Fix powRgrip toolholding system uses a taper-to-taper, press-fit collet holding design that creates a vibration-damping gap to interrupt the strength and severity of vibration waves.

Three components make up the powRgrip: holders, collets and press-fit assembly mounting units. Toolsetting is accomplished in no more than ten seconds without heat or hydraulics as used in other tool clamping systems. The powRgrip technology allows tools to be used immediately after the loading cycle concludes without the limitations and tool-life compromises of traditional clamping units.

Rego-Fix will have the ECR team's NTT IndyCar Series racecar on display for attendees to experience up close and in person. The powRgrip toolholding system plays a key role in the team overcoming the unique challenges of high-speed machining operations. With the use of the company's toolholders, ECR has maintained precision and critical surface finishes, extended tool life, minimized tool runout and shortened cycle times for its productive part processing.

ECR is able to machine parts at full 24,000 rpm spindle speeds, which would be impossible without the powRgrip. As a result, jobs that once took two or three weeks to fulfill are now completed within a couple of hours.

regoUSA.com

Ceratizit

FOCUSES ON NEXT-GENERATION TOOLING, SUPPLY CHAIN STRENGTH AT IMTS 2026

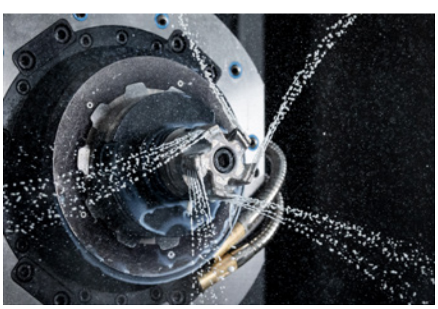

At IMTS 2026, Ceratizit will feature digital twin technology, a broad range of cutting tool innovations, and the company's supply chain independence. Located in the West Building, Booth #431900, Ceratizit will highlight how the convergence of digital solutions, tooling innovation and supply chain control allows manufacturers to navigate increasingly complex production demands.

Ceratizit USA will bring its visual twin to Chicago for the show. Programmed and designed specifically for guests at IMTS, the visually driven digital twin will bring tooling solutions and real-world industry applications to life.

In addition, a key highlight at IMTS will be the continued expansion of its advanced line cutting tools portfolio, including Sacramento-produced inch end mills that complement the established metric range. Available in four-, five-, six-, seven- and nine-flute configurations, the end mills are engineered to deliver stable performance across a wide range of applications.

Attendees will also see a range of recently introduced solutions, including the MaxiMill–211-DC, WTX UNI and WTX Quattro drills in both inch and metric, the MonsterMill–ISO-S solid carbide end mill, and the MaxiMill–S-Power face milling platform.

Further, as part of the Plansee Group, Ceratizit will demonstrate its position to ensure continuity of supply to IMTS guests. Through vertically integrated carbide production and a global manufacturing network, the company maintains consistent quality and availability even amid ongoing market volatility and supply chain disruptions.

"Manufacturers need high-performance tools and confidence in their supply chain," said Troy Wilt, managing director of Ceratizit USA, Cutting Tools Division. "At IMTS, we're demonstrating how our control over carbide production, combined with application-driven tooling, helps customers stay competitive."

ceratizit.com

Kuka Robotics

HIGHLIGHTS ADVANCED ROBOTICS AT IMTS 2026

Kuka Robotics will showcase its advanced robotic automation solutions for machine tool tending, material handling and robotic milling with the company's OEM and integration partners at IMTS 2026. Visitors to Booth #236807 in the North Building will experience live demonstrations that showcase how Kuka is making automation easier and how its industrial robots, autonomous mobile platforms and partner technologies work together in real-world production environments.

Kuka will highlight robotic machine tool automation through a series of integrated demonstrations featuring multiple CNC machine tool OEM partners. These applications will include EMAG, Matsuura and SYIL machines, each paired with a standardized Kuka robotic system to deliver flexible machine-tending solutions that simplify deployment across a range of production environments.

For enhancing ease of operation for job shops, the SYIL machine tool will leverage Siemens *Sinumerik* software with Kuka's *mxAutomation* to enable seamless control of both the CNC machines and Kuka robots from a single interface. Kuka will also demonstrate a full-service automation model in collaboration with Formic Automation to highlight how manufacturers can adopt robotic machine tending through a scalable, service-based approach that reduces complexity and supports evolving production needs.

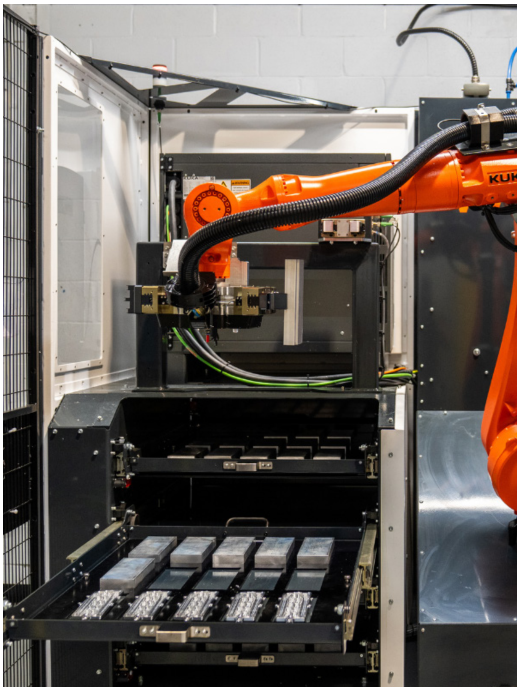

As part of the machine tending demonstrations, Mairotec's MairoFlex Compact 8 system, which features Kuka's KR Cybertech nano robot and AI vision technology, will pick large-diameter parts from a randomly assorted bin and place them onto the portable trays of Kuka's autonomous mobile platform, the KMP 600P. The system will then demonstrate automated machine tool tending by transporting the tooling to a lathe to illustrate a standardized robotic solution that combines 3D bin picking, mobile automation and seamless machine interaction within a single production cycle.

Kuka's material handling and finishing demonstration will showcase a fully integrated, multistep process developed in collaboration with Specialty Tooling Systems (STS). The KR Titan ultra industrial robot will lift and position a large, heavy cast part, demonstrating high-payload handling capabilities for demanding industries such as automotive and heavy machinery. Supporting the process, the KMP 3000P will autonomously transport the part to a robotic finishing cell, where the KR Titan will position it for processing.

The KR Fortec MT will then perform a robotic grinding application using advanced tooling to showcase high-performance surface finishing of large components.

Kuka will also demonstrate advanced robotic machining processes from Kuka Systems, featuring the KR Quantec nano in a high-precision milling application. This demonstration highlights how robotic machining continues to evolve as a flexible and accurate solution for complex part production, enabling manufacturers to improve consistency, reduce manual intervention and adapt more easily to changing production requirements.

Additionally, attendees at IMTS can experience a live presentation on "CNC Driven Robotics: How Siemens and Kuka are Simplifying Automation for the Modern Shopfloor" with Ron Bergamin, key technology manager for machine tool automation at Kuka, and Tiansu Jing, senior product manager at Siemens. The presentation takes place on Tuesday, September 15 at 11 a.m. CST in room W192-A.

kuka.com

United Machining

LAUNCHES LIMITED-EDITION WIRE EDM, 5-AXIS MILLING MACHINE MODELS

United Machining North America has launched limited-edition models of its wire EDM and milling machines.

Agie Charmilles has launched the Cut E 350 Prime and the Cut E 600 Prime, limited-time offerings in its Cut E wire EDM series. It features Turbo Tech onboard cutting technology and the Uniqua HMI.

"We are thrilled to introduce the Cut E 350 Prime and the Cut E 600 Prime, two stellar offerings in the Agie Charmilles lineup," United Machining North America President Onik Bhattacharyya said. "Both of these machines combine the equipment and software that the brand is known for with an attractive price point and robust service package. You can set your watch to the precision and reliability you will have on your floor."

Not to be outdone, Mikron Mill has launched the Mill E 700 U Prime, a special edition of its 5-axis Mill E Series. This machine brings a 20,000 rpm Step-Tec spindle that boasts 120 Nm of torque and 36 kW of power.

"There are so many incredible features in the Mill E 700 U Prime, including the high-performance spindle that comes standard, the Heidenhain control and the integrated or third-party automation," Bhattacharyya said. "But what I'm most excited about is that this machine will give an entirely new segment of manufacturers access to the day-in, day-out accuracy and efficiency that Mikron Mill and Swiss-made machining provides."

gfms.com

Tormach

INTRODUCES AUTOMATIC COLLET CLOSER FOR 8L LATHE, BOOSTING SPEED, PRECISION FOR SMALL-PART PRODUCTION

Tormach introduced a new Automatic Collet Closer for its 8L Lathe, delivering faster part changes, more consistent clamping and improved workflow efficiency for machinists producing small, precision components.

Designed exclusively for the 8L Lathe, the Automatic Collet Closer provides air-actuated clamping for standard 5C collets and integrates with Tormach's PathPilot control system. Clamping force is controlled by regulating input air pressure, allowing users to achieve repeatable, adjustable part retention without the need for manual drawtube operation. The system is manufactured in the U.S. and offers optional foot pedal actuation for added operator control and faster hands-free operation.

The addition expands the capabilities of the 8L Lathe, a compact CNC-ready platform designed for prototyping, short-run production and toolroom work. Built to bring professional-grade turning capabilities to small shops, educational environments and product development teams, the 8L combines precision, ease of use and broad tooling compatibility in a machine that operates on standard single-phase power.

"Customers will be most excited about how much faster part and collet changes become with the Automatic Collet Closer," said Reid Halvorsen, mechanical design technician at Tormach. "Adjustable air pressure at the FRL gives users precise control over clamping force, making it easy to securely hold everything from standard parts to thin-walled or delicate components."

By eliminating manual tightening, the system helps reduce repetitive operator tasks while improving consistency across runs, particularly in applications requiring frequent part swaps, small-batch production or careful handling of delicate materials. The air-actuated design also enables more repeatable setups, helping machinists maintain part quality while reducing downtime between operations.

"This has been one of the most requested accessories for the 8L, and for good reason," said Max Sample, technical presales advisor at Tormach. "The Automatic Collet Closer saves time and simplifies daily operation by removing the need to manually tighten the drawtube. With air-actuated 5C collet clamping, loading and unloading parts is faster, easier and more consistent."

tormach.com

ABB Robotics

LAUNCHES NEW AUTOMATED SURFACE FINISHING CELL

ABB Robotics launched its first fully automated sanding and polishing cell, the OmniVance Collaborative Surface Finishing Cell, empowering a new wave of manufacturers to automate key surface finishing tasks, such as sanding and polishing.

"A growing number of companies are looking to automate processes such as sanding and polishing, but many smaller businesses lack in-house robotics expertise—so while they need to deliver perfect quality every time, until now, many have not had a solution that fits their needs," ABB Robotics Managing Director of Business Line Industries Craig McDonnell said. "Many businesses are wary of investing in complex, bespoke automation, while off-the-shelf tools lack the scalability and capability they require. With our new OmniVance Collaborative Surface Finishing Cell, we're introducing

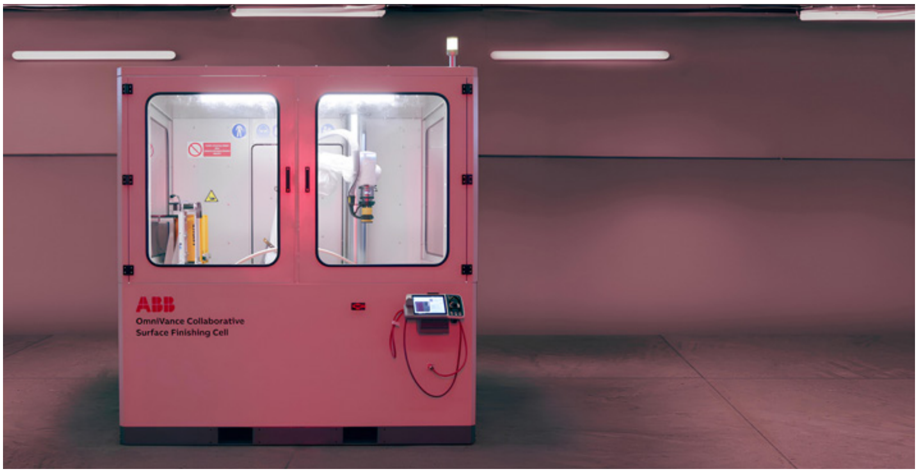

industrial-grade robotics in a simple, affordable and scalable solution."

ABB Robotics' OmniVance Collaborative Surface Finishing Cell bridges the gap between customized automation and entry-level tool kits with its turnkey solution, using a GoFa collaborative robot to execute high-quality, precision surface finishing, without the need for robotics expertise.

The cell is entirely self-contained, delivered as a complete plug-and-play solution, including the GoFa cobot and safety components. The fully CE-certified cell does not require any additional engineering to switch on and begin production, and the easy addition of new tools and accessories makes it highly adaptable in high-mix environments.

By automating repetitive sanding and polishing tasks, the cell increases throughput and reduces the traditional scrap and rework, saving time, effort and costs, according to the company. Integrated dust extraction readiness helps maintain a clean, healthy work environment while further enhancing finished product quality. Automation also reduces physical strain and frees skilled workers to concentrate on more valuable tasks.

Matching the new cell's industrial-grade quality and efficiency is its operational simplicity, enabled by ABB Robotics' intuitive software developed to govern the entire finishing process. Its tablet-style interface is user-friendly for those without robotics expertise and needs no custom programming. Features such as lead-through 3D path recording, 2D preset path creation and intuitive path editing, integrated into Wizard Easy Programming blocks, can reduce programming time by up to 90 percent.

The OmniVance Collaborative Surface Finishing Cell demonstrates how collaborative robots can deliver application-specific solutions that boost competitiveness, even for businesses and operators who are new to robotics.

abb.com/global/en/areas/robotics

The Doctor Is In

Inside Luftex's five-pillar approach to gearbox repair

Aaron Fagan, Senior Editor

Case crush and tooth fracture on a helical pinion is the kind of damage that demands engineering analysis before anyone starts cutting replacement gears. **(Image: Luftex)**

Most gearbox repair follows a familiar sequence. A unit shows up damaged, the shop measures what's worn, makes replacement parts, reassembles, and ships it back. Scott Franks, P.E., spent decades inside that world at Lufkin Industries and came to believe it wasn't enough.

In 2015, Franks and his partner, Albert Stokley, opened Luftex Gears in Lufkin, TX. They built the company around a structured four-pillar service model—Inspect, Analyze, Advise, and Produce—that put engineering analysis ahead of production. A gearbox that arrived at Luftex didn't go straight to the shop floor. It went through engineering first.

"Our time at Lufkin Industries is where we learned the value of customer relations through inspecting, analyzing, advising, and producing to ultimately complete the repair," Franks says. What pushed them to go independent was the 2013 GE acquisition of Lufkin Industries. "The GE philosophy towards customer relations didn't align with ours, so we decided to provide an alternative choice to customers who value involvement through Luftex."

Luftex had no OEM product line and no installed base. Everything depended on the expertise of its people. During those startup years, Franks took seven days off in five years. Operators became CNC technicians. Managers and engineers doubled as ground crews and janitors. Everyone learned to drive a fork truck.

Inspection in Two Modes

Luftex's inspection work splits into in-plant evaluation of running equipment and shop analysis of failed units. In-plant inspections look for signs of proper lubrication supply, acceptable contact across tooth flanks, and any evidence of metal distress. Scheduled periodic inspections add a trending layer: has the contact pattern shifted? Has noise increased? Have bearing clearances changed?

"If caught early enough, mitigation processes can be successfully implemented," Franks says.

When a failed unit arrives at the facility, inspection starts with what Franks calls a "30,000-foot evaluation," associating major damage with probable causes. Then the unit goes through an engineering analysis to verify the design against AGMA or ISO standards before root cause work begins.

For gearboxes that arrive without original documentation—common in older steel, mining, and sugar operations—reverse engineering starts in conversation with the customer, not at the measurement table. "The name plate on the gearbox doesn't affect how the components react when in operation," Franks says. "What's important is how a gearbox reacts to the conditions it sees while running at the required service load, speeds, and operating environment." The analysis may lead to recommended changes in bearing design, gear geometry, or lubrication—well beyond like-for-like replacement.

"There are numerous facilities with gear cutting machines that can offer to manufacture a gear but with little ability to analyze the validity of a design," Franks says. "It is this service that Luftex can provide that many companies offering gear or gearbox repair cannot support."

Adding a Pillar: Educate

During the startup years, Luftex operated under four pillars but didn't have the bandwidth to formalize training as a service. The 2019 acquisition by Sumitomo Drive Technologies changed that. Sumitomo absorbed the administrative overhead and freed Luftex's people to focus on production, continuous improvement, and formal customer education.

Today, Luftex hosts several two-day gear schools each year and offers customized on-site training. The curriculum starts with the foundation—checking that it's solid, flat, free of burrs, and making full contact with the bottom of the gearbox housing. From there, it moves to verifying proper alignment between mating rotating elements to ensure load distribution, coupling setup (different methods for different gear designs), and unit startup checks covering lube pumps, oil flow, temperatures, and recommended inspection and documentation frequency. Franks describes attendees having "ah ha" moments when a discussion topic connects to a recurring problem back at their plant—root causes that turn out to be alignment issues, foundation problems, or lubrication regimes that were wrong from the start.

"A company's culture has a tremendous effect on how open the communications are between a supplier and owner when trying to establish what caused a failure," Franks says. "Sumitomo intends to engage customers who value an honest relationship that leads to a partnership that benefits both parties."

Analyze, Advise, and the Honesty Question

Having Sumitomo behind Luftex gives the analysis stage a depth most independent shops can't match. Franks describes cases where a customer installed a competitor's gearbox and immediately had reliability issues. Luftex's analysis revealed the units were originally undersized for the application and the original housing wasn't large enough to make the necessary modifications required for a reliable design. In extreme cases like this, the only fix is a properly rated Sumitomo OEM replacement.

The advise stage is where that analytical depth pays off in practice. Luftex presents options with the strengths and weaknesses of each: a temporary repair that buys time while a permanent solution is planned, a long-term repair with investment in spare critical components, or a new unit if repair costs exceed replacement. Sometimes a repair wins even when a new unit is cheaper, because delivery lead times on new equipment may not fit the customer's downtime window.

"Sumitomo Drive Technologies has the means to offer multiple options to a customer and help them decide what best fits their needs," Franks says.

The Bearing Arrangement Nobody Caught

One case shows the full model at work. A steel plant customer had recurring low-speed gear tooth failure at roughly eighteen-month intervals. About a third of the tooth was broken out in several locations around the gear, and the pattern repeated across multiple units at different plant locations.

Luftex ran gear ratings on every pinion and gear. Each reduction carried a significant service factor—the gears should not have been failing. Because the damage was limited to a third of the tooth length, something was causing misalignment in the mesh and poor load distribution. Deflection calculations came back well within acceptable limits. Housing bores measured parallel. Multiple locations ruled out bad foundations.

The root cause: the tapered roller bearings on the low-speed gear were oriented in the same direction, an atypical arrangement. Under axial thrust loading, the bearings unseated, creating additional clearance that let the shafts drift out of parallel. The load migrated to one end of the mesh and fractured the teeth.

Luftex redesigned the housing for a new bearing arrangement. More than ten years later, the units are still running.

For Related Articles Search

failure analysis

at geartechnology.com

Better Gears Coming Back

Luftex's gear grinders do more than restore worn surfaces. Profile and lead modifications improve the misalignment factor in gear rating formulas, increasing the service factor over non-modified sets. Improved surface finish raises the probability of developing a full elastohydrodynamic oil film between mating teeth.

On materials, Luftex limits its steel suppliers to a small number of partners with a track record of producing clean steel that hardens to greater depths. "We base our ratings and repairs on high AGMA grades of steel, so by developing partnerships with only a few quality suppliers who understand our specifications, we eliminate the risk of having inferior steel end up in our repairs," Franks says. Today's grades support higher allowable stresses than what was available when many of these gearboxes were built. A repair using current materials can transmit more horsepower or operate at a larger service factor than the original unit.

The Workforce and the Future

Franks doesn't dodge the industry's long-term problem: fewer people want to do this work. He compares the aftermarket gearbox business to auto repair—there are dealership shops that service one brand, and independent shops that fix whatever rolls in. Luftex was built as an independent shop, where the learning curve is steeper, and experience matters more.

"The gear business has gotten labeled as a 'dirty' business that isn't as glamorous or high tech as other careers," he says. "I don't think that's a totally fair assessment." Luftex trains its engineers and technicians on the engineering and mechanics of gearbox operation, but Franks is direct about the limits of formal instruction. "Even with that engagement, experience plays a huge role in becoming competent," he says.

Since the acquisition, Luftex's new office building in Lufkin has added 1,200 square feet dedicated to learning and development. The installed base of Hansen and Paramax gearboxes gives the aftermarket business a foundation of OEM service work. The general repair heritage gives it range.

The five pillars, in the order Franks now lists them: Inspect, Analyze, Educate, Advise, and Manufacture. "Six years into the Sumitomo acquisition of Luftex," he says, "the support to continue these pillars in our daily offerings only gets stronger."

us.sumitomodrive.com/en-us/luftex-lufkin-industrial-gearbox-repair-rebuild-services

Automotive Brain Power

Four Key Takeaways from CTI Symposium USA 2026

Matthew Jaster, Director, Editorial Content

***Delegates from Stellantis, Linamar, McLaren, Horse and Stellantis discuss the future of hybrid technology at the CTI Symposium USA 2026 in Novi, MI.* (All images: Matthew Jaster)**

One of my favorite events each year is the Car Training Institute (CTI) Symposium USA in Novi, MI. The program brings together engineers to discuss and debate the current state of the North American automotive market from a powertrain, transmission, and electrification perspective.

Recently, many U.S. automakers have retracted their "all-in" EV strategies while others continue to promote a multifaceted approach where internal combustion engines (ICE), battery electric vehicles (BEV), plug-in hybrid electric vehicles (PHEV), range extended electric vehicles (REEV) and full and mild hybrids all have a place at the architectural layout table.

Our kind CTI host and chair, Patrick Lindemann, president, e-Mobility and chassis mechatronics, Americas, Schaeffler Group USA Inc., said it best when he compared the 2026 North American auto market to the Wild West. "You wake up one morning and you really don't know what direction the industry is going."

Lindemann promised two full days of legislation, technology, and engineering advancement discussions as well as a much-needed wake-up call on the China dilemma. He also didn't shy away from the potential complacency that has taken place across the U.S. automotive industry regarding China.

"Is the China threat a wake-up call to get better and faster? Did we get a little bit lazy over the years? I mean, in the old days, everything was remarkably simple and clear, right? Today, it's not as easy as it looks to figure out what the consumer wants."

1. A Diverse Vehicle Portfolio

Market forecasts say ICE, hybrids, range extenders, and all-electric vehicles will all play a role in the auto industry through 2040. Ingo Scholten, CTO, Horse Powertrain, said these are the products that will be sharing the roads in the next 15 years. "We're obligated to make these vehicles as good as possible. It's no longer a question of picking a single solution but focusing on all the solutions available. What design elements from commercial electric drive vehicles can we bring to the U.S. automotive market? What areas do hybrid teams need to focus on in the future? The consensus is electrification is still the way forward but how fast before we truly get there? The key will be collaboration and ingenuity."

2. The EREV Alternative

If the initial costs of EVs (as well as range anxiety) still frightens consumers, extended-range electric vehicles (EREVs) continue to be a gateway to full battery electric vehicles. In standard range extenders, a combustion engine drives the electric motor, charges the high-voltage battery and extends the range. This continues to be a popular alternative to BEVs as these vehicles remain independent of the messy charging infrastructure. Trucks and large SUVs have the necessary space for both powertrains, but the jury's still out on other vehicle segments. EREV models coming out in 2026-2028 include the Ram 1500 REV, Nissan Rogue e-Power, Ford F-150 Lightning EREV, Audi SUV EREV, Ram EREV SUV, Jeep Grand Wagoneer REEV and more.

3. The China Dilemma

The U.S. automotive road map has little time to figure things out before China comes knocking down the door with a plethora of efficient and cost-effective automobiles just waiting for the average American consumer to test drive. However convoluted or messy the current automotive industry looks like today in America, it's scarier to think about what it could look like ten years down the road. The Chinese are competing across several industrial segments. They own the cars, the battery technology, they own their own shipping fleets to deliver vehicles across the globe. They're capable of delivering more than a million vehicles worldwide.

"The thing that makes China formidable competitors is that they're highly vertically integrated. The best example of this is BYD, not only do they make their own batteries, their own battery cells, their own processing capabilities, but they see North America as the final prize," said Michael Dunne, Dunne Insights. "Here in the West, the saying "win-win" means both parties win, right? What does "win-win" mean in Chinese? It means China wins twice."

If we look at Tesla as an example, Dunne said two years ago Elon Musk said Tesla was no longer an EV company. They became an AI and robotics company. Why did he do that? He knew nobody could go toe-to-toe with the Chinese on cost or price. Nobody can do it. The only way to stay ahead in the automotive market is through dramatic innovations, not incremental changes or upgrades. Dunne said we need to do more than just make X percent improvements to hybrid powertrain efficiency, for example.

"Who do the Chinese fear and admire the most? Tesla. Musk has created an amazing company, vertically integrated, supercharger stations. He has his own batteries. He's got a lithium refinery. The thing that the Chinese spirit admires the most is in our own backyard, but we were like, 'no, no, that's Tesla.' There's so much we could learn from them. Just look at what Tesla's doing and model that. That's what the Chinese do. Innovation is the way forward, "Dunne said.

4. Automotive Brain Power

The companies that refused to put all their eggs in one electrification basket are the companies that have a better path toward future growth and success in automotive.

"We've continued to solidify our portfolio via new engines even for high performance vehicles, or to support electrified powertrains. We continue to expand and push out the hybrid system across the entire lineup," said Jordan Choby, group vice president, powertrain engineering, Toyota. "The hybrid is becoming really our core, right? We have been able through continuous evolution of that system, via cost performance, driving engagement, etc. to create a great value proposition for the customer."

Micky Bly, senior vice president, propulsion systems, Stellantis, said engineers must take a Rubik's Cube approach to the automotive market today. "We need to take every type of powertrain technology today and study the various combinations. Maybe the EV solution is the potential path to simplify some of these challenges, but you should not overreact in the short term."

The threat from China, however, doesn't need to cause panic if the engineering teams continue to do what they do best here in North America.

"We don't crawl under a rock and hide, right? China is a competitor, a worthy competitor. Let's start by leading in powertrain technology. It's still just physics. How do you produce an engine? How do you convert the energy and transmit it down to the wheels? What are the advantages of powering the vehicle electrically or mechanically along the way? Globally, the goal is to provide the most competitive technology we can in this space," Bly added.

Knowledge is power and both Bly and Choby strongly agree that the entire Chinese automotive ecosystem should be examined—the engineering technology and speed alone should be cause for concern. The amount of automation and robotics being utilized inside their plants is staggering. Bly said, "China has blinding fast cycle times." And even with the fastest cycle times, the engineers are still not happy with the numbers. They plan to drop cycle times even more by the end of 2026.

The U.S. automotive market needs to work on the engineering technology, really lean-in on the automation capabilities and see where AI and robotics can add even more value to the production lines.

Michael Dunne, Dunne Insights, discusses the 2026 Chinese automotive industry outlook.

During Dunne's presentation on China, he recommended that the engineers go to Canada or Mexico and see how these Chinese vehicles run and operate and the technology they're leaning in on. The goal is to see how the Rust Belt can be the innovators, technophiles and champions in powertrain and drivetrain technology for years to come.

The CTI Symposium was a room full of gearheads and engineers, but also people directly involved with the entire automotive supply chain. China's ability to keep costs down and see their investments paying off is something everyone in that room needs to understand and pay attention to moving forward.

Bly learned a lot from his visits to automotive plants in Asia. "We're not going to win this race on human power; we're going to win this race with brain power."

The CTI Symposium is one great example of why face-to-face technical events are still so important and relevant to the future success of manufacturing and engineering.

"I love this conference. I've said it many times. This is one of the last hardcore technical powertrain gatherings," said Bly. "There's only a few left and this is one that continues to be important and relevant to the industry, especially for the driveline and propulsion team members."

cti-symposium.world

Optical vs. Tactile Gear Measurement for E-Mobility

A practical comparison of fringe projection and conventional tactile systems for classic and waviness gear characteristics

Roman Groß, Carl Zeiss Industrielle Messtechnik GmbH and Dr.-Ing. Ânderson Schmidt, Robert Bosch GmbH

The use of electric drives seems to be a promising solution due to their high efficiency and optimized driving dynamics. However, they receive special attention in terms of noise behavior, as the engine noise of a combustion engine is no longer present. This can have a big impact on user comfort, especially at low speeds. The noise level of gears is, among other things, influenced by their design and manufacturing process. For this reason, in addition to the already established gear parameters evaluation, features are also tested that provide indications of possible frequencies from the manufacturing process that can lead to noise during operation. In addition to frequency testing in its spectrum and amplitude, the analysis of the topography of the tooth flank surface is becoming increasingly important. Surface analysis using waviness parameters is an important tool for understanding the causes of noise generation. For this purpose, it is necessary to measure the tooth flanks in several measuring planes in profile and helix direction. This type of measurement is currently mostly carried out with tactile measuring systems, which can lead to long measurement times, depending on the design parameters of the gear. In this project, a practical measurement comparison of conventional tactile and optical systems was done. The goal was to investigate if and how good the measurement results of classic characteristics and waviness characteristics of the different physical measurement principles are comparable. In addition, it was determined whether the use of optical fringe projection measurement systems is suitable for gear metrology.

Project Overview and Task Description

Conventional measurements with tactile systems are time-consuming and provide limited information about the surface quality of a gear. Optical measurements enable a supposedly more comprehensive information base to establish a correlation with the noise, vibration, and harshness (NVH) behavior of the tooth flank. To evaluate an optical measurement system for measuring the entire tooth flank surface and correlating the surface properties with the NVH behavior, two Centers of Competence (CoCs) of Robert Bosch GmbH have joined forces. The CoCs Optical and Non-Destructive Metrology (OND) and the CoC Gear Set Manufacturing (GSM) have been working on this two-year project (StraTec 23-036 Optical Gear Quality Evaluation) since January 2023. As part of the first phase of the project, extensive research was carried out in digital information sources as well as in scientific literature. In addition, expert interviews were conducted, and selection criteria for potential systems and providers with potential were defined. Due to the initial identification of ten small and large companies as well as research institutes, a reduction in effort was made by selecting six candidates for initial test measurements. At the beginning of 2024, the project had to be discontinued by Robert Bosch GmbH. Of the six selected candidates, only two had begun intensive investigations on a specified measurement object by this time. The tactile measurement data provided by Zeiss correlated very well with internal tactile measurement results. Zeiss signaled its willingness to continue the optical comparison measurements even after the project had been stopped, which resulted in this joint report.

A gear pump (hereinafter referred to as Bosch-Shaft) was chosen as the object of study, which was manufactured by means of a continuous generating grinding process. In the selection of the study object, properties were deliberately considered to pose a challenge for optical measurement methods, both from the literature and from in-house experience. These include reflections of the tooth flank surface and limited accessibility, especially in the protuberance area of the gearing. For a full capture of a tooth with optical measuring systems, several measuring positions are necessary (stitching), which means additional potential measurement uncertainty contributions.

Description	Symbol	Value
Number of teeth	z	12
Normal module	m_n	≈ 3 mm
Facewidth	b	30 mm
Profile shift	$x \cdot m_n$	≈ 0,75 mm
Normal pressure angle	α_n	≈ 20,0°
Helix angle	β	0°
Reference diameter	d	36,0 mm

Table 1—Geometry data of the Bosch-Shaft.

For the comparison measurements, a spur gear was used. Due to the profile shift and the protuberance, this gear already represents a medium to difficult accessibility for optical

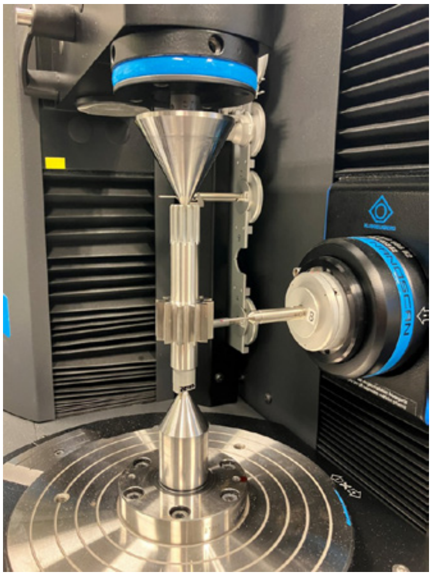
Figure 1—Klingelnberg P40.

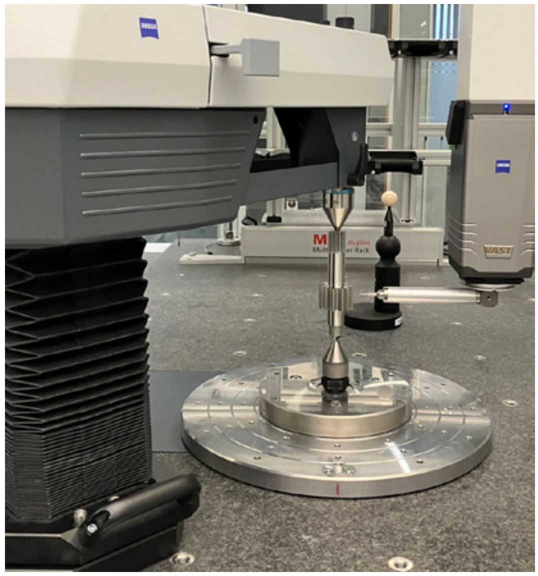
Figure 2—Zeiss Prismo verity.

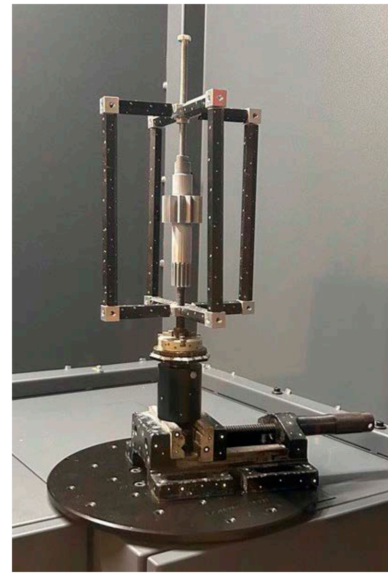
Figure 3—Zeiss Atos Q.

measuring systems and was evaluated as a suitable study object. The geometry data of the gear can be found in Table 1.

To ensure comparability with the results, a detailed task description was created. This includes all relevant aspects such as the definition of the reference elements and the reference system, the number of measuring points, the filter settings, as well as the relevant characteristics and tolerances. Two tactile measuring systems from different manufacturers and an optical measuring system were used for comparison measurements. The tactile measuring systems used were a Klingelnberg P40 gear measuring instrument (GMI) (Ref. 1), available at Bosch (test setup see Figure 1), and a Zeiss Prismo Verity coordinate measuring machine (CMM) with tailstock (Ref. 1) (test setup see Figure 2). As a representative non-contact optical measuring system, a Zeiss Atos Q fringe projector was used in a Zeiss ScanBox 4105 (test setup see Figure 3).

The procedure for the comparison measurements was divided into two steps. In step 1, a tactile system comparison of the existing Klingelnberg GMI with a Zeiss CMM was carried out. This comparison served firstly to validate the tactile measurement results obtained by the Klingelnberg GMI with the tactile measurement results obtained from the Zeiss CMM and, secondly, forms the basis of the measurement and evaluation strategy for the non-contact optical measurement system from Zeiss. In the following chapters, the measurement results are divided into two main blocks: *Classic characteristics* and *waviness characteristics*. Classic characteristics refer to all determined characteristics according to ISO 1328-1:2013-09; for better presentation, the individual characteristics have been summarized in the main categories *profile, helix, pitch,* and *runout*. In addition, depending on the workpiece, *tooth thickness values* such as *spanwidth* and *measurement over two balls* were compared with each other. *Waviness characteristics* are understood to be the orders with the corresponding amplitude (O/a), determined from the order spectrum using the compensating sine method (Ref. 2) and the helix angle of waviness (β_w) (Ref. 3). The measurement results presented in the following chapters result from several repeatability measurements per measuring system. At least ten repeatability measurements were carried out and compared with each other according to the mean value per characteristic and system.

Bosch-Shaft Tactile System Validation

The measurement scope on the Bosch-Shaft with twelve teeth included an all-tooth measurement of all profiles and helices, including the pitch and runout measurement (or extraction of the pitch points from the profile data), as well as the measurement of tip and root circles on all teeth. In addition, one tooth was measured topographically with twenty-one profile sections.

In the first step, the tactile measurement results of the Klingelnberg P40 were compared with those of the Zeiss Prismo verity. For a better visual and numerical comparison of the measurement data, the function *actual-actual comparison* (Ref. 4) of the Zeiss *Gear Pro* involute gear metrology software was used. Figure 4a shows the actual-actual comparison data as an example for the classic characteristic profile for the measurement data of Klingelnberg P40 (green) and Zeiss Prismo verity (blue). The color coding is retained throughout the report. Even when the results are greatly enlarged and exaggerated, the very good comparability of the measurement data of both tactile measuring systems can be seen in Figure 4b.

In the table of Figure 4a, the numerical differences (Δ) of the individual characteristics are shown. For all determined

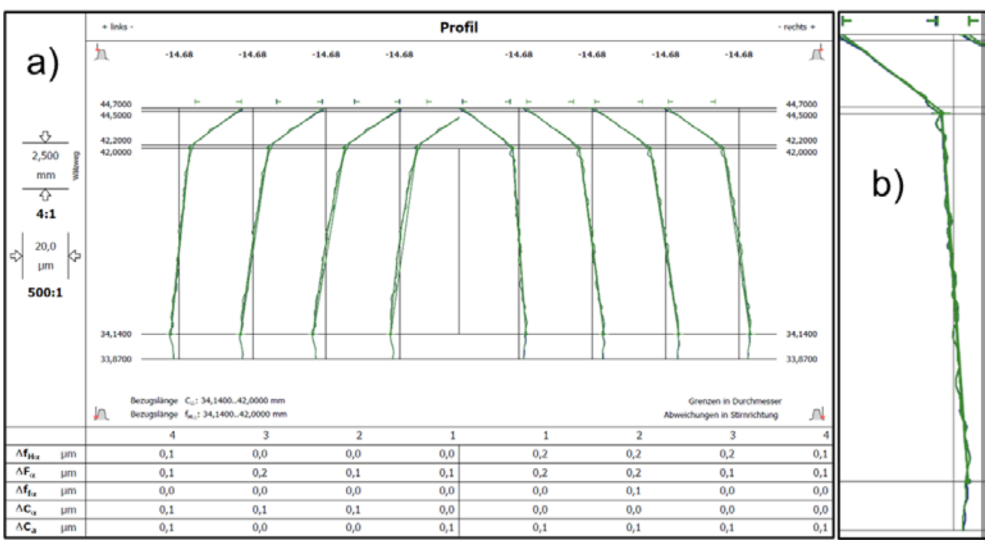

Figure 4—Actual-actual comparison profile Bosch-Shaft Tactile: a) overview and b) enlarged.

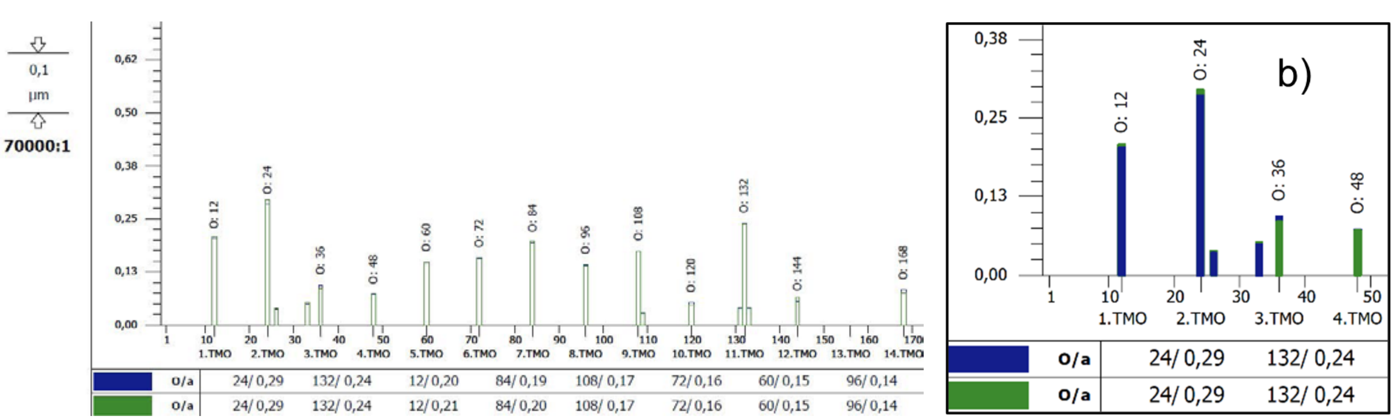

Figure 5—Actual-actual comparison order spectrum profile Bosch-Shaft Tactile: a) overview and b) enlarged.

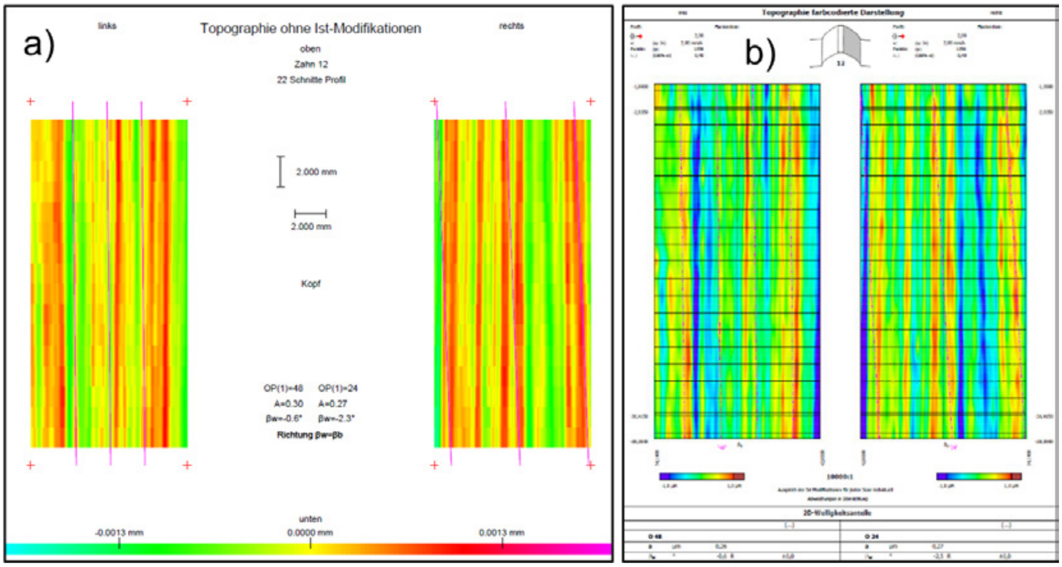

Figure 6—Color-coded topography Bosch-Shaft Tactile: a) Klingelnberg P40 and b) Zeiss Prismo verity.

characteristics of profile and helix the differences are Δ < 0.5 μm. In the determined characteristics of pitch, runout, and spanwidth, the respective differences are Δ < 1.5 μm.

Figure 5a shows the actual-actual comparison for the waviness characteristic order spectrum as an example of the profile measurement data. Figure 5b shows the very good comparability of the tactile measuring systems, which is enlarged and highlighted in color. The differences Δ are also visible in numerical form on the measurement report and were in the range Δ < 20 nm.

The actual-actual comparison is not suitable for comparing the waviness characteristic helix angle of waviness (β_w). For this purpose, the respective measurement reports of the color-coded topography by Zeiss and Klingelnberg were visually compared with each other. The differences Δ of the determined helix angles of waviness were in the range Δ < 0.5° (Figure 6).

Bosch-Shaft Tactile/Optical Comparison

The physical measuring principle of fringe projection is fundamentally different from the tactile measuring principle. The physical limitations and special topics of optical measurement methods were discussed in detail in VDI Report No. 2393, 2021 (Ref. 5). The very good comparability of the tactile measurement results from section 2 was classified as sufficiently accurate for the system validation. The measurement and evaluation strategy of Zeiss Prismo verity was thus defined as the basis for the evaluations with Zeiss Atos Q. The special feature of the *Gear Pro* involute gear metrology software from Zeiss is that the same measurement program can be used for the evaluation of non-contact measurement data in STL format as for tactile measurement. This offers the advantage that, despite the different physical measurement principles, no further uncertainty contribution regarding the measurement strategy must be considered. In principle, however, as shown in Ref. 5, various restrictions must be observed for a high-quality measurement. The following relevant points are to be mentioned as examples: spraying-in of the surface to minimize reflections; ensuring accessibility in areas that are difficult for optical systems, such as the tooth root or the transition area to the protuberance; and sufficiently high point density to minimize the influence of polygonization (merge individual scans into a final mesh), see Figure 7.

The measurement scope for evaluating the Bosch-Shaft with twelve teeth has remained identical to that used for the tactile validation measurements when evaluating the optically determined data with the Zeiss Atos Q. However, there is a significant difference in the recording of measuring points. For the subsequent mathematical evaluation regarding gear characteristics, the complete recording of the workpiece is necessary. Depending on the number of teeth, generating the data set takes significantly longer than tactile measurement with a GMI or CMM. An overview of the measurement scope and the measurement times is shown in Table 2.

	Klingelnberg P40	Zeiss Prismo verity	Zeiss Atos Q
Measuring principle	Tactile	Tactile	Optical
Scope of measurement	All-tooth measurement 12 teeth profile / helix / pitch / runout / tip circle / root circle / topography 1 tooth 21 intersections		
Dataset size point cloud STL	-	-	145 MB
Preparation	1 min	1 min	10 min
Dataset creation	-	-	8 min
Measurement time	14 min	15 min	3 min
Total time	15 min	16 min	21 min

Table 2—Bosch-Shaft tactile/optical measurement scope and measurement times.

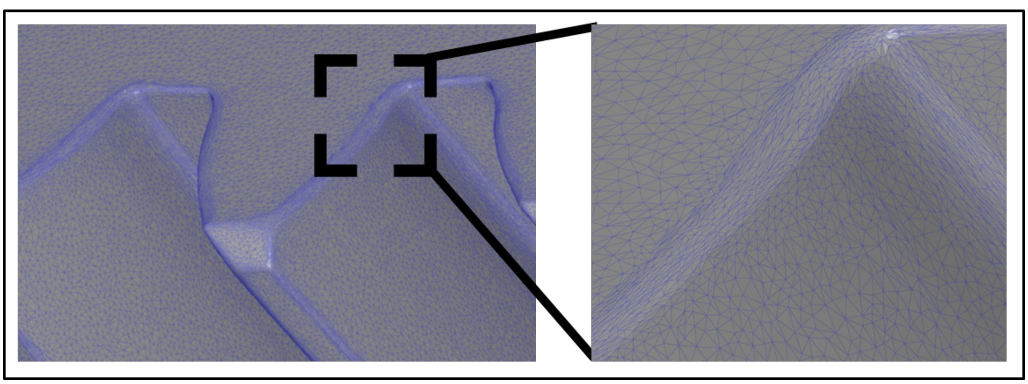

Figure 7—Measurement point density and STL data model after polygonization.

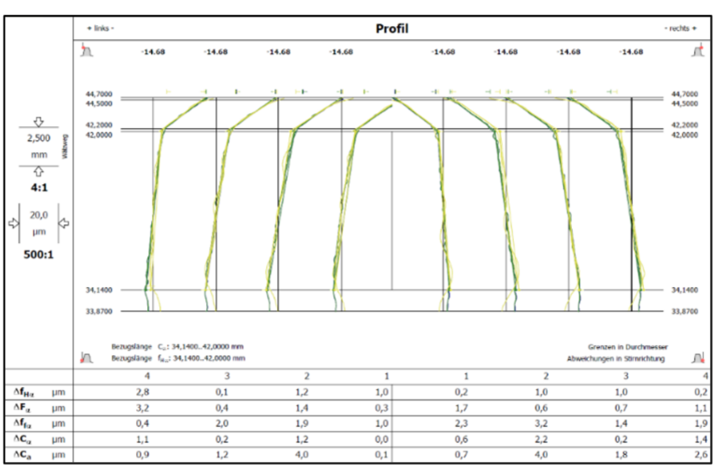

Figure 8—Bosch-Shaft tactile/optical actual-actual comparison profile.

The differences in the measurement results are again displayed using the actual-actual comparison function in the same way as in the section "Bosch-Shaft Tactile System Validation." The classic characteristic profile is shown as an example in Figure 8 for the measurement data of Klingelnberg P40 (green), Zeiss Prismo verity (blue) and Zeiss Atos Q (yellow).

The system-related lower measuring point density of the fringe projection generates, especially in profile direction, rounding in edge areas due to polygonization and thus leads to falsification of the measurement result. At the Bosch-Shaft, there are only about 100 points in the profile direction after polygonization. Figure 9 visualizes the profile comparison results from Figure 8, enlarged for fringe projection systems' "critical" edge areas after polygonization and gear evaluation, transition area involute zone into profile tip relief, and transition area into root zone/protuberance.

For all determined characteristics of profile and helix, the respective differences are Δ < 6 µm. For the determined characteristics of pitch, runout, and spanwidth, the respective differences are Δ < 3 µm. The differences determined are thus within the known orders of magnitude of tactile/optical comparison measurements of gears (Ref. 5).

The differences for the waviness characteristic order spectrum are shown as an example for the profile measurement data in Figure 10. In Figure 10b, you can see the noise of the order spectrum of the measurement data determined by fringe projection (yellow) in the low-frequency range and the lack of detection of orders in the high-frequency range in an enlarged and colored variant. This makes it difficult to reliably detect frequencies. The numerical differences in the orders found are in the range Δ > 50 nm.

The comparability of the waviness characteristic helix angle of waviness (β_w) for the largest order found is shown in Figure 11. The differences between the two tactile measurement results and the optical measurement result are in the range of Δ < 1.5°. In Figure 11, there is a visual comparison of the optical system given, but it is presented in a "damped" way. The reason for the visual differences can be explained by the noisy result of the order spectrum; the physical system-related restrictions cannot be dismissed out of hand at this point. The differences determined by the tactile system validation and the tactile/optical comparison are summarized in Table 3.

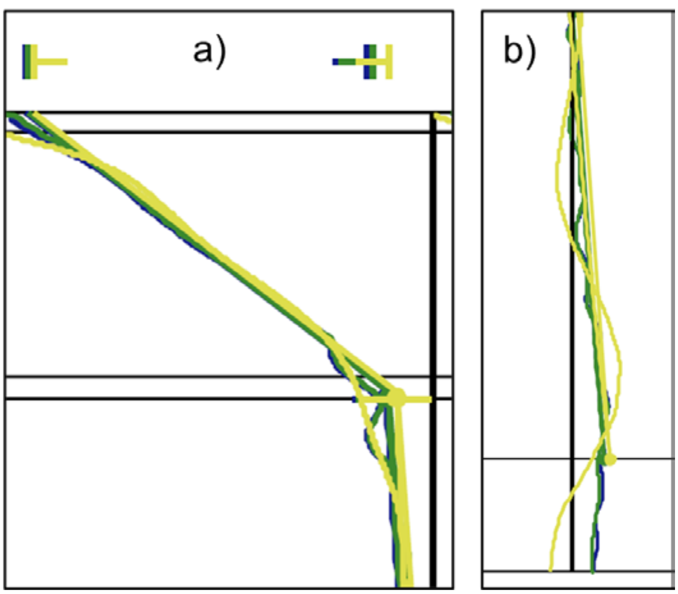

Figure 9—Bosch-Shaft tactile/optical actual-actual comparison profile enlarged: a) tip and b) root area.

Step number:	1. Tactile system validation	2. Tactile/optical comparison
Classic characteristics		
Profile	Δ < 0.5 µm	Δ < 6 µm
Helix	Δ < 0.5 µm	Δ < 4 µm
Pitch	Δ < 1 µm	Δ < 2 µm
Runout	Δ < 1.5 µm	Δ < 3 µm
Spanwidth	Δ < 1.5 µm	Δ < 3 µm
Waviness characteristics		
Order spectrum O/a	Δ < 20 nm	Δ > 50 nm
Topography β_w	Δ < 0.5°	Δ < 1.5°

Table 3—Measurement results Bosch-Shaft tactile/optical.

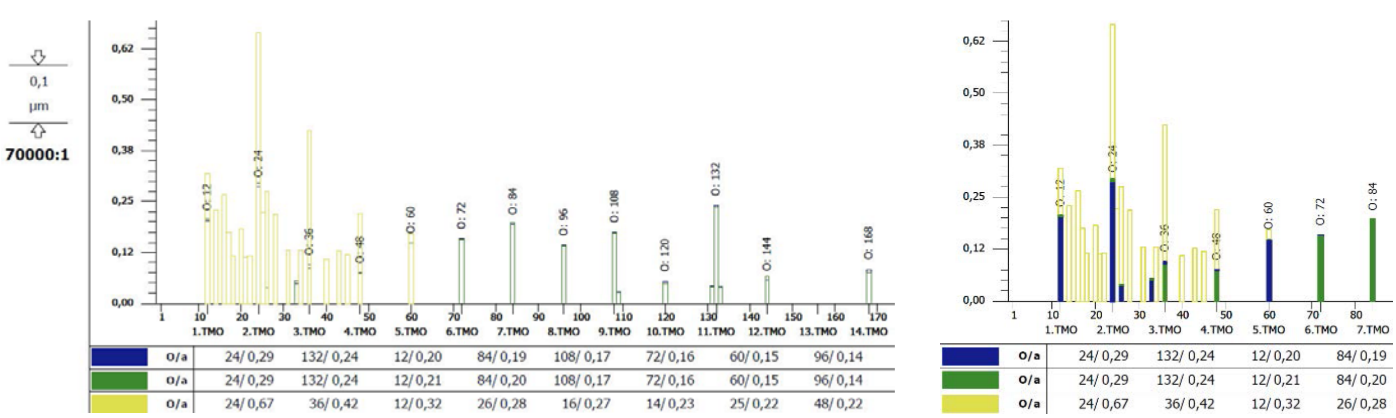

Figure 10—Bosch-Shaft tactile/optical actual-actual comparison order spectrum profile: a) overview and b) enlarged.

FVA Involute Waviness Artifacts Tactile/Optical Comparison

Since there were no conspicuous waviness on the Bosch-Shaft, but the question of reliable detection of waviness characteristics, with fringe projection systems for Bosch was in the foreground, two waviness artifacts from the Forschungsvereinigung Antriebstechnik e.V. (FVA) from the project FVA involute waviness artifacts (Ref. 6) could be used for the comparison. The two waviness artifacts are grinded artifacts with specifically applied waviness of different orders (Figure 12). Both waviness artifacts are helical external gears with: number of teeth (z) 37, normal module (m_n) 1.75 mm, and facewidth (b) 40 mm. For the tactile/optical comparison, the waviness artifact B1 (order 37, 1. Tooth Mesh Order [TMO]) and D1 (order 45, 1. TMO ± 8) were available. In the FVA research project no. 733 I, twelve tactile Klingelnberg GMI were used to determine the waviness applied by production technology in a ring comparison in 2018. The amplitudes of the waviness were in a range < 0.5 µm.

For the results presented below on the two FVA involute waviness artifacts, the same methods, repeatability measurements, and results presentations were used as described in the sections "Bosch-Shaft Tactile System Validation" and "Bosch-Shaft Tactile/Optical Comparison" for the Bosch-Shaft Table 4 shows the measurement scope and the measurement times. The differences of all determined characteristics are shown in Table 5.

As an example, Figure 13 shows the waviness characteristic order spectrum profile of the FVA involute waviness artifact B1 for the measurement data of Klingelnberg P40 (green), Zeiss Prismo verity (blue), and Zeiss Atos Q (yellow).

In Figure 14, the color-coded topography plots for the visualization of the waviness characteristic helix angle of waviness (β_w) of the FVA involute waviness artifact B1 are shown, in Figure 15, correspondingly, for the FVA involute waviness artifact D1.

Figure 12—FVA involute waviness artifact B1.

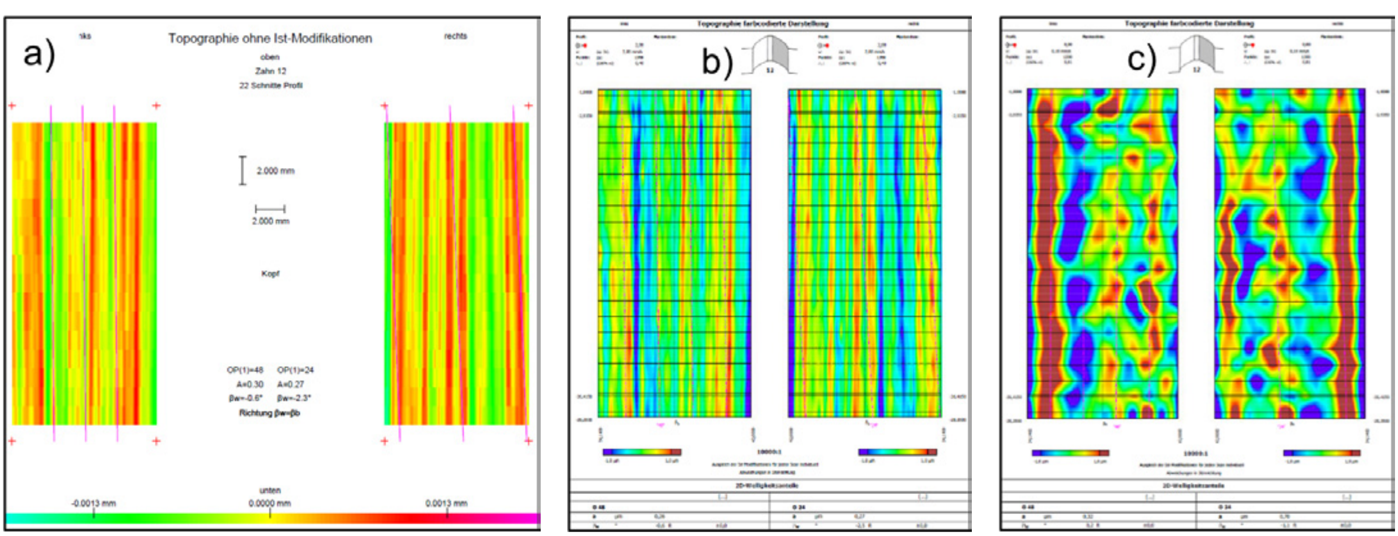

Figure 11—Color-coded topography Bosch-Shaft tactile/optical: a) Klingelnberg P40, b) Zeiss Prismo verity and c) Zeiss Atos Q.

	Klingelnberg P40	Zeiss Prismo verity	Zeiss Atos Q
Measuring principle	Tactile	Tactile	Optical
Scope of measurement	All-tooth measurement 37 teeth profile / helix / pitch / runout / tip circle / root circle / topography 1 tooth 31 intersections		
Dataset size			
point cloud STL	-	-	450 MB
Preparation	1 min	1 min	20 min
Dataset creation	-	-	18 min
Measurement time	31 min	30 min	5 min
Total time	32 min	31 min	43 min

Table 4—Tactile/optical measurement scope and measurement times for FVA involute waviness artifacts.

Step number:	1. Tactile system validation	2 Tactile/optical comparison
Classic characteristics		
Profile	$\Delta < 0.5$ µm	$\Delta < 4$ µm
Helix	$\Delta < 0.5$ µm	$\Delta < 4$ µm
Pitch	$\Delta < 0.5$ µm	$\Delta < 2$ µm
Runout	$\Delta < 1$ µm	$\Delta < 3$ µm
Spanwidth	$\Delta < 1$ µm	$\Delta < 3$ µm
Waviness characteristics		
Order spectrum O/a	$\Delta < 50$ nm	$\Delta < 200$ nm
Topography β_w	$\Delta < 0.5°$	$\Delta < 1°$

Table 5—Tactile/optical measurement results FVA involute waviness artifacts.

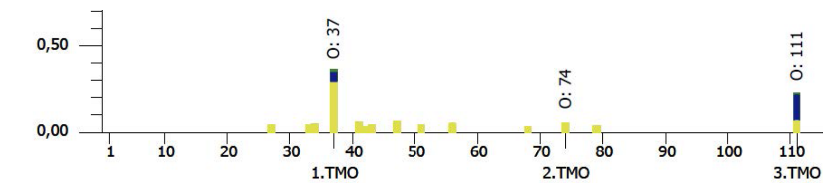

(blue)	O/a	37/ 0,34	111/ 0,22	74/ 0,05	148/ 0,04	185/ 0,04
(green)	O/a	37/ 0,36	111/ 0,22	74/ 0,05	148/ 0,04	185/ 0,04
(yellow)	O/a	37/ 0,29	47/ 0,06	111/ 0,06	41/ 0,06	74/ 0,05

Figure 13—Tactile/optical actual-actual comparison order spectrum profile FVA involute waviness artifact B1: a) overview and b) enlarged.

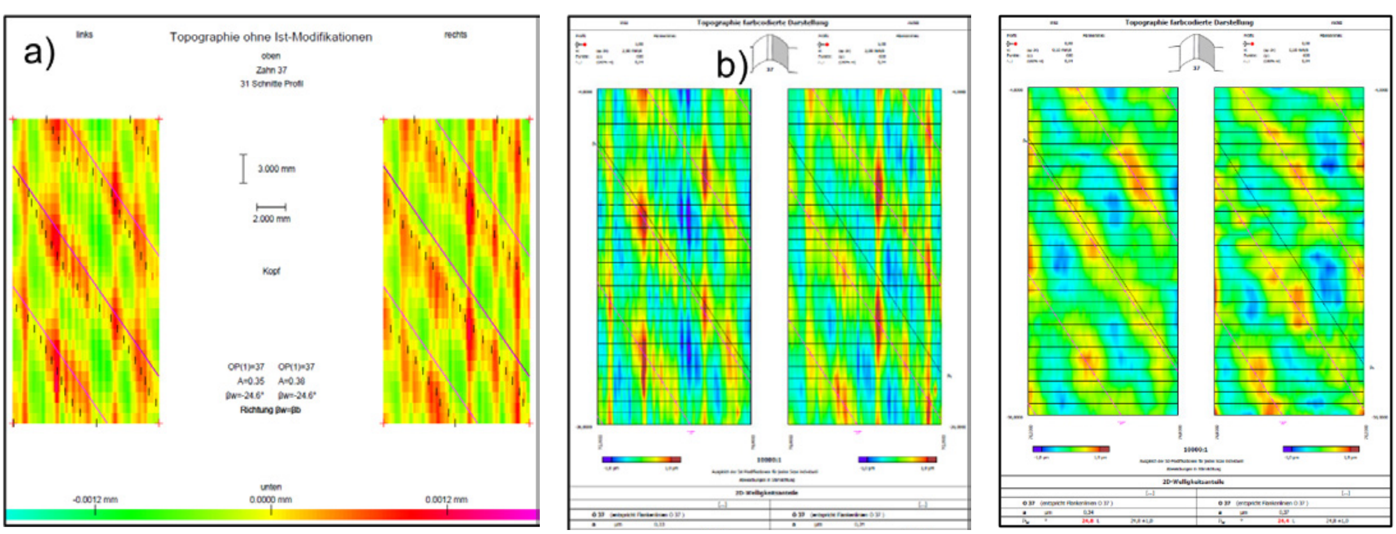

Figure 14—Tactile/optical color-coded topography FVA involute waviness artifact B1: a) Klingelnberg P40, b) Zeiss Prismo verity and c) Zeiss Atos Q

The results obtained on the FVA involute waviness artifacts tend to be comparable to those on the Bosch-Shaft, and even significantly better for some characteristics, since the surface quality of the artifacts is of higher quality than that of the Bosch-Shaft.

Note: The aim of this investigation with regard to the FVA involute waviness artifacts was primarily to analyze a suitable measurement object with specifically applied waviness with different measuring systems and not to achieve comparability with the FVA research project no. 733 I, since the detection of the helix angle of waviness (β_w) was not part of the investigation in the FVA project at that time.

Summary and Conclusion

The use of fringe projection measuring systems for gear metrology is generally suitable. However, the suitability depends heavily on the measuring object. Classic characteristics are comparable to tactile measuring systems in the range of Δ < 5 µm, and in some cases, much more accurate in the range of Δ < 3 µm. Regarding waviness characteristics, suitability can be assessed as conditional. If orders are found, they are quite comparable in the range of 50 < Δ < 200 nm to the amplitudes found by tactile systems. However, noise in the low-frequency range of the order spectrum and the partial lack of detection of orders in the high-frequency range can lead to misinterpretations regarding the noise analysis. On the other hand, the very good comparability of the helix angle of waviness (β_w) is remarkable. Both the Bosch-Shaft and the FVA involute waviness artifacts were comparable to tactile measurement results in the range of Δ < 1° to 1.5°. Basically, the causes of differences between optical and tactile measurement results can be found in the physical measurement principle itself. The issue of orthogonal accessibility in tooth spaces and generally accessibility in internal gears limits suitability. In addition, the working distance and the measuring field used influence the measurement point density. The subsequent polygonization of the individual scans of fringe projection measurement systems negatively impacts the measurement result, especially in edge areas, as it results in rounding effects. Regarding gears, these are primarily the transition areas from the root or protuberance area to the main involute area, as well as the transition from this to the tip relief or tip chamfer area. The effect is a potentially strong influence on the regression elements in the sub-areas, which primarily affects the calculation of profile and helix slope deviations (and thus also on the profile and helix total deviations). Likewise, of course, on the calculation of the regression elements in the relief areas, if existing. Additional efforts, such as spraying-in and cleaning the measurement objects as well as the attachment and removal of reference marks, have a primary effect on the total measurement time and only in a subordinate way on the measurement results. This can certainly be optimized for series measurements by means of fixtures and spraying devices. In contrast to the above-mentioned points, one of the strengths of fringe projection is definitely the possibility of additional visualization options such as a holistic color-coded nominal/actual comparison, if a CAD model of the gearing is available. Since a complete STL data model of the gear is always available for the determination of gear characteristics, the measurement scope can be adjusted at any time, also after the measurement process itself. For example, in the event of a gearbox failure, the data of individual gears could be re-evaluated for additional analyses and also with additional detailed topographical evaluations. Fringe projection thus primarily offers added value as a supplementary tool for development and analysis. Special features of the measurement software from Zeiss are, on the one hand, the possibility that the same measurement programs from *Calypso* and *Gear Pro* can be used for tactile and optical measurements with an identical measurement and evaluation strategy, and on the other hand, the advantage that an all-tooth measurement is not necessarily required to determine the helix angle of waviness (β_w) (Ref. 4).

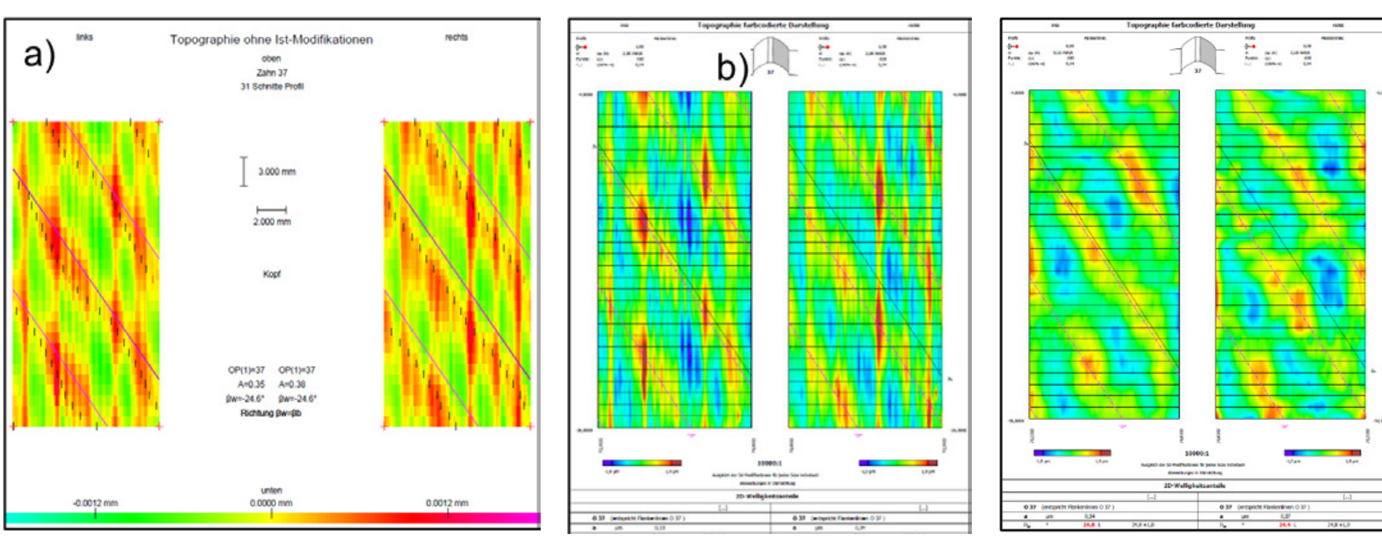

Figure 15—Tactile/optical color-coded topography FVA involute waviness artifact D1: a) Klingelnberg P40, b) Zeiss Prismo verity, and c) Zeiss Atos Q.

Acknowledgement

Special thanks go to Mr. Matthias Fath from HAW Hamburg and Dr. Stefan Groß as well as to the Arbeitskreis Messtechnik of the Forschungsvereinigung Antriebstechnik e.V. for providing the two FVA involute waviness artifacts. Many thanks also to Prof. Dr.-Ing. Günther Gravel for his support in the preparations of the comparison measurements.

zeiss.com/metrology

bosch.com

For Related Articles Search

`optical metrology`

at geartechnology.com

References

1. Groß, R.: „Vergleich verschiedener Messmethoden in der Verzahnungsmesstechnik – Messen zwischen Spitzen als Hybridsystem neu gedacht", 7. VDI-Fachtagung Verzahnungsmesstechnik 2021, Nürnberg – VDI-Berichte Nr. 2393.
2. Gravel, G.; Seewig, J.: „Welligkeitsanalyse von Verzahnungsmessungen", 3. VDI-Fachtagung Verzahnungsmesstechnik 2008, Leonberg – VDI-Berichte 2053.
3. Gravel, G.; Kahnenbley, T.: „Neue Entwicklungen zur Welligkeitsanalyse akustisch auffälliger Verzahnungen", 6. VDI-Fachtagung Verzahnungsmesstechnik 2017, Leonberg – VDI-Berichte 2316.
4. Kunzmann, S.: „Mathematischer Ansatz und die Realisierung von Welligkeitsanalyse-Werkzeugen", 8. VDI-Fachtagung Verzahnungsmesstechnik 2024, Nürnberg – VDI-Berichte 2440 ISBN-Nr.: 978-3-18-092440-3 (E-ISBN-Nr.: 978-3-18-102440-9).
5. Groß, R.: „Vergleich verschiedener Messmethoden in der Verzahnungsmesstechnik – Kunststoffzahnräder auf Koordinatenmessgeräten und berührungslosen Mess-systemen", 6. VDI-Fachtagung Verzahnungsmesstechnik 2017, Leonberg – VDI-Berichte Nr. 2316.
6. FVA Stirnrad-Welligkeitsnormale, Forschungsvorhaben Nr. 733 I, Heft 1308, 2018.

Systems Failure

Rethinking failure, replacement, and supply strategy in heavy industry

Pamilanga Ltd.

Figure 1—Early-stage surface fatigue and distress on a heavy-duty gear tooth flank. Surface damage may progress well before catastrophic failure becomes visible. **(All Images: Pamilanga Ltd.)**

In heavy industry, gears rarely fail in the dramatic way people imagine. More often, there is no broken tooth, no immediate seizure, and no single event that clearly marks the beginning of the problem. What appears to be a healthy gear may already be operating with edge loading, unstable lubrication film, progressive surface fatigue, or overload at the tooth root. By the time visible damage becomes obvious, the failure mechanism has usually been active for some time. This matters because plant decisions are still too often made at the component level. A gear is inspected, damage is found, and attention immediately shifts to material quality or OEM replacement. In practice, however, most serious gear incidents are system-driven. Alignment condition, shaft and housing stiffness, bearing clearance, lubrication regime, thermal growth, start-stop duty, shock loading, and maintenance response all influence the way the tooth pair actually carries load. Understanding that distinction changes not only how failures are diagnosed, but also how replacement strategy should be managed. Once a critical gear is out of service, the challenge is no longer purely technical. The question becomes how to restore reliability quickly, with controlled risk, and without accepting unnecessary dependence on long OEM lead times.

Failure Often Starts Long Before Fracture

Early-stage gear distress is typically progressive rather than catastrophic. Micropitting is one of the clearest examples. Under mixed or boundary lubrication, local asperity contact causes repeated surface fatigue at a very small scale. The damage may first appear as a dull grey patching effect on the active flank, usually near the pitch line or in areas where contact has shifted away from the intended load zone. Operators may continue running because the gear still looks serviceable and the machine has not yet tripped. But once the surface is disturbed, local stress concentration increases and the damaged area tends to grow.

Scuffing is different in appearance and mechanism. It is associated with lubricant film collapse combined with sliding under load, often during transient events such as hot restarts, contamination, high bulk oil temperature, or inadequate viscosity at operating conditions. Instead of fine fatigue damage, the tooth shows tearing, smearing, and directional scoring. Bending fatigue, by contrast, develops from repeated tensile stress at the tooth root. If the effective load distribution across the face width is poor, root stress rises sharply at one side, and cracks may initiate from the fillet long before a full tooth breakage occurs.

The key lesson is that visible damage type is only the surface expression of the real operating condition. A gearset may show micropitting because the lambda ratio is too low for the actual duty, because the contact pattern has moved toward one edge, or because load spikes are repeatedly pushing the pair beyond its intended regime. A correct diagnosis, therefore, requires the gear to be viewed as part of a dynamic system, not as an isolated manufactured part.

Material Is Often Blamed First

Material quality and heat treatment certainly matter. Case depth, flank hardness, core strength, cleanliness, grinding burn, residual stress, and geometry quality all affect life. But in field investigations, these factors are often blamed too early because they are easier to discuss than system behavior. A replacement gear can be metallurgically sound and still fail

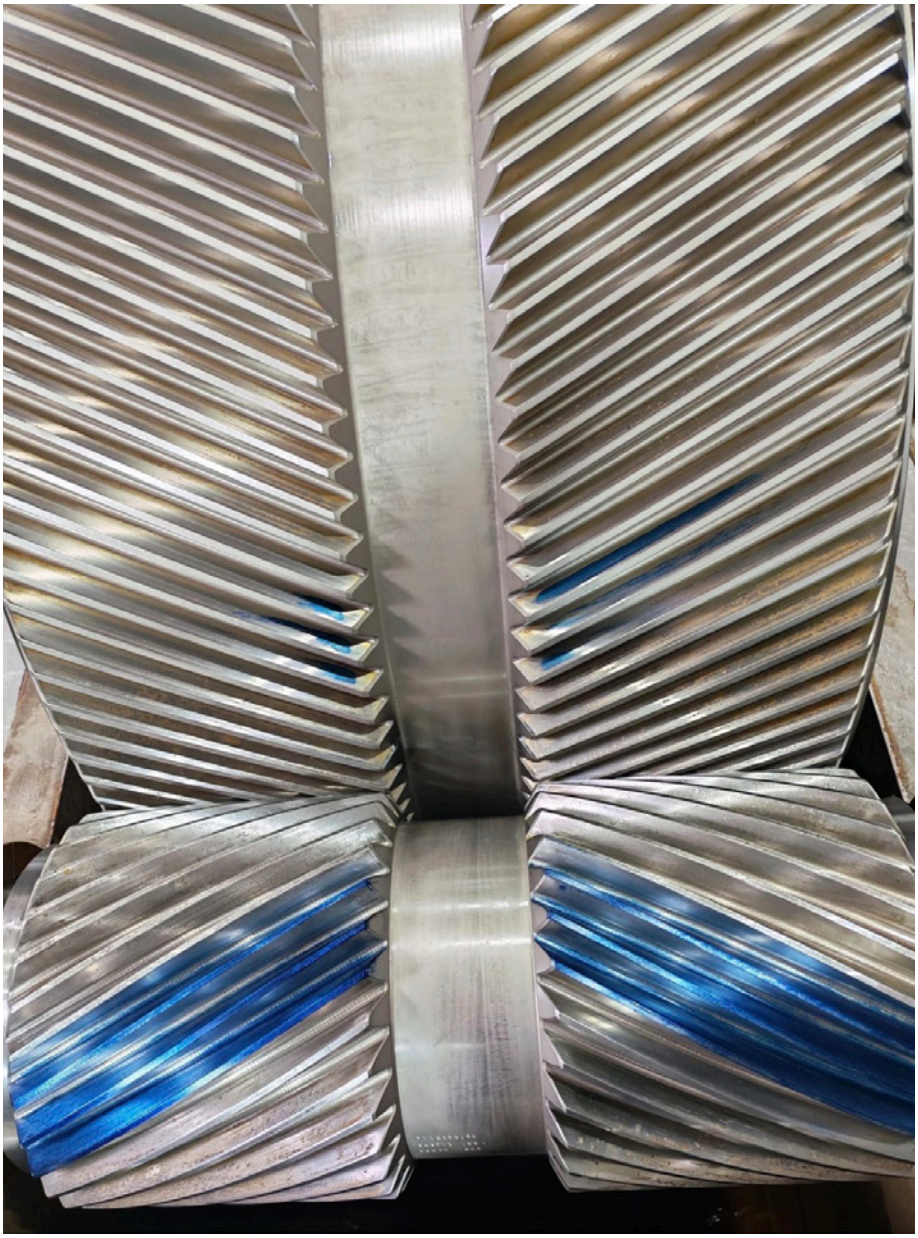

Figure 2 — Contact pattern verification on helical gear teeth. Blue marking compound highlights the actual contact area across the tooth flank. Uneven patterns may indicate edge loading, alignment deviation, or load distribution issues before visible gear damage occurs.

Failure mode	What it looks like in service	What usually drives it
Micropitting	Grey frosting, matte patches, early surface fatigue on active flank	Low film thickness, edge loading, roughness mismatch, contamination, repeated load cycling
Scuffing	Smearing, tearing, directional score marks, rapid local distress	Lubricant film collapse, high sliding, temperature excursion, poor viscosity control
Macropitting / spalling	Larger pits or flake-like surface removal	Progressed surface fatigue, overload, inadequate hardness or case support, misalignment
Bending fatigue	Root crack initiation, tooth fracture after repeated cycles	High root stress, poor load distribution, overload events, fillet stress concentration

Table 1—Typical failure modes and what they usually indicate.

Fine Grinding Circuits—Wear, Efficiency, and the Wrong Simplifications

A similar pattern appears in fine grinding circuit decisions. In mineral processing discussions, equipment selection is often reduced to a simple efficiency comparison between ball mills and vertical grinding technologies. In reality, the decision is again system-dependent. Ball mills are sometimes dismissed as old technology, yet they remain highly effective where robust operation, predictable particle-size control, and tolerance to variable feed are more important than headline energy claims.

In abrasive services such as silica-rich duty, wear behavior becomes a central design variable. Vertical configurations can offer attractive energy performance, but the wear environment on rollers, tables, or other grinding surfaces may become the limiting factor in practice if the ore or industrial mineral is highly abrasive. Ball mill circuits paired with appropriate classification, liner selection, and media strategy often remain the preferred solution where product fineness must be controlled reliably, and wear risk has to be managed conservatively.

The point is not that one machine type is universally superior. It is that equipment should be selected according to the real operating constraint: energy, wear, maintenance interval, product-size distribution stability, or project execution risk. Just as with gears, the best engineering decision emerges when the component is evaluated in the context of the full duty.

early if the real problem lies in the way load reaches the teeth.

Misalignment is the most common hidden amplifier. It does not have to be dramatic to be damaging. A contact pattern that migrates toward one side of the face width creates local overload, changes the oil film behavior, and raises tooth root stress. The source may be shaft deflection under torque, pedestal movement, bearing wear, housing distortion, soft foundation response, assembly error, or thermal growth between cold alignment and hot operating conditions. In large mill drives and heavily loaded reducer stages, this distinction is critical: the measured alignment at standstill may not represent the alignment under process load.

Lubrication must also be treated as a system variable rather than a maintenance checkbox. Oil cleanliness, viscosity selection, additive chemistry, temperature stability, spray pattern or bath level, and actual flow to the mesh all matter. Technically correct oil can still perform poorly if contamination rises, the nozzles miss the mesh, or operating temperature drives viscosity below the intended range. When film thickness falls, the tooth surface begins sharing load through direct asperity contact, and fatigue accelerates.

This is why experienced investigators usually ask four questions before discussing replacement: What is the actual contact pattern under load? What changed in the machine before the damage was noticed? What do oil condition and vibration trends show? And has the train been checked as an assembled system rather than as a collection of separate parts?

What a Practical Field Assessment Should Include

A useful field assessment does not begin and end with photographs of damaged teeth. It should combine surface observation, geometry checks, operating evidence, and surrounding machine condition. On the tooth flanks, inspectors should review the active contact pattern, the position and direction of distress, the extent of end loading, and whether wear is uniform across the set. Backlash values should be recorded rather than estimated, and radial or axial runout should be checked where possible. In repaired or long-running units, wear pattern history can be as informative as a one-time measurement.

Supporting evidence from the machine is equally important. Bearing clearances, shaft journal condition, coupling status, housing fastener security, foundation behavior, and machine base integrity all influence the mesh. Oil should be reviewed not only for contamination and viscosity but also for wear debris trend, water ingress, and signs of thermal distress. Vibration data, if available, may show rising gear-mesh activity, sidebands related to modulation, or changes in 1x shaft response that point back to alignment and support condition.

For high-consequence assets, the best investigations convert observations into a decision matrix: continue with monitoring, repair in place, re-machine selected parts, or replace the gearset and correct the surrounding system drivers. That last point is essential. Replacing a gear without addressing the reason it was distressed simply resets the clock.

The Real Operational Problem: Replacement Under Pressure

Once serious damage is confirmed, plant priorities change immediately. Engineering may still want root-cause certainty, but operations will focus on uptime, production loss, and restart risk. In this phase, OEM dependency becomes a major constraint. For critical gears used in mills, high-load reducers, and heavy-duty transmission systems, original replacement lead times can extend from several months to much longer, depending on size, heat treatment route, pattern availability, and backlog. Even where price is accepted, time may not be.

This is where many organizations face an uncomfortable gap between theoretical preference and practical recovery. Waiting for the original source may be the simplest administrative answer, but it is not always the best risk decision. If the plant is losing production weekly, the true cost of replacement is not only the purchase price of the gear. It is the combined effect of downtime, temporary workarounds, maintenance exposure, and the possibility that the new gear will enter the same operating condition that damaged the previous one.

A better response framework separates two questions that are too often blended together: first, can a replacement be manufactured outside the OEM channel to the required technical standard, and second, what additional checks are necessary to ensure the system does not re-create the same failure mode? Once those questions are separated, alternative sourcing becomes a technical and project-management exercise rather than a compromise.

Alternative Manufacturing Is Viable if Qualification Is Disciplined

Alternative manufacturing should never mean copying a damaged part blindly. The process must begin with disciplined reverse engineering and qualification. First, the gear geometry needs to be captured correctly: module or diametral pitch, pressure angle, helix angle if applicable, face width, tooth count, profile modifications, root geometry, mounting interfaces, and any relevant fit or runout conditions. Three-dimensional scanning can help, but it is not enough by itself. Damaged or worn teeth can distort the digital picture, so direct measurement and interpretation by gear specialists remain essential.

Second, the material and condition of the original part must be understood. Depending on the component, this may include chemistry verification, hardness mapping, case-depth evaluation, microstructure review, and crack inspection. The objective is not simply to identify what the previous gear was made from, but to understand whether that specification was appropriate for the duty. In some cases, the best replacement is a like-for-like reproduction. In others, the better choice is to preserve geometry while improving process control, grinding quality, cleanliness, or heat treatment consistency.

Third, manufacturing route and inspection plan must be aligned with application risk. Blank production method, machining sequence, heat treatment route, flank finishing, balance if relevant, non-destructive testing, and final gear metrology all need to be defined before production begins. A qualified supplier should be able to show not only that it can machine a gear, but also that it can control lead error, profile error, pitch accuracy, hardness, and distortion across the full process. This is particularly important for large gears where heat treatment and final finishing introduce significant variability if not managed closely.

Finally, replacement planning has to include installation and startup discipline. Contact checking, alignment verification, lubrication readiness, controlled commissioning, and early inspection intervals are part of the replacement strategy not an afterthought. A technically correct gear installed into an unchanged misaligned train is still a vulnerable gear.

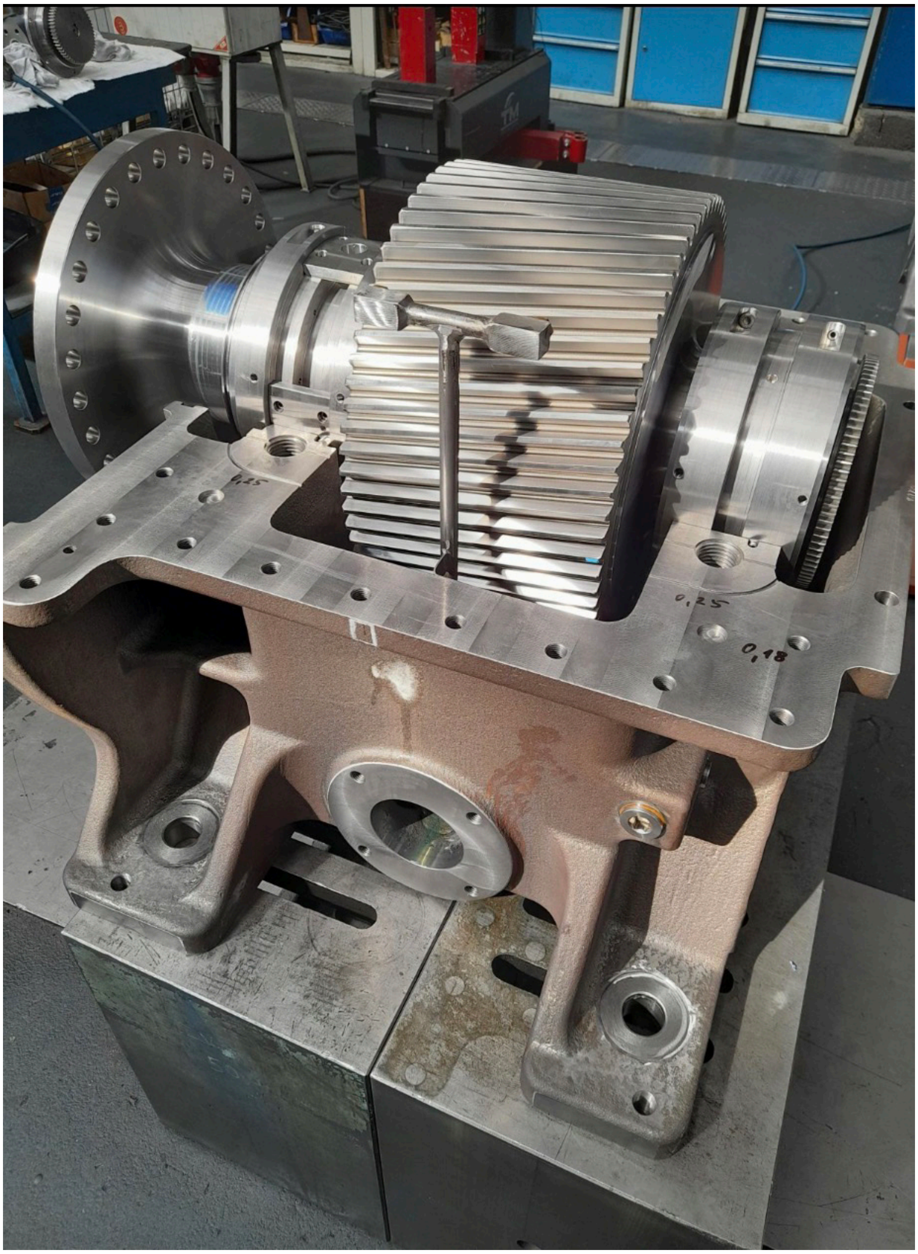

Figure 3 — Gearbox assembly under inspection. Heavy-duty gear and shaft assembly during fitting and inspection. Long-term reliability depends on evaluating the complete system rather than replacing the gear alone.

Step	What must be confirmed
Geometry capture	Tooth form, helix or spur geometry, profile modifications, interfaces, fits, and allowable runout
Material verification	Chemistry, hardness, case depth where relevant, microstructure, crack status, and previous distress evidence
Design validation	Load path review, service condition check, and confirmation that the reproduced design suits actual duty
Manufacturing plan	Blank route, machining, heat treatment, grinding or finishing, and distortion control sequence
Inspection package	Gear metrology, NDT, hardness results, dimensional report, and release criteria before shipment
Installation and startup	Alignment under realistic condition, contact pattern, lubrication readiness, and controlled run-in or early follow-up inspection

Table 2—Qualification checklist for non-OEM replacement.

Representative Field Case: Heavy-Duty Mill Drive

The following anonymized case reflects a pattern commonly seen in heavy-duty mill drives. A plant identified progressive flank distress on a critical drive gear after operators reported increasing noise during load changes. There was no tooth breakage and no immediate trip event, but inspection showed visible micropitting concentrated away from the intended central contact zone, together with signs of uneven load across the face width. Initial reaction focused on whether the gear material had been inadequate.

A broader review changed the picture. Contact evidence suggested recurring edge loading. Further checks found that bearing condition and support behavior had allowed the mesh to operate differently under process load than during static alignment. Oil condition was serviceable but not ideal, and the combined effect was enough to push the flank into an unfavorable lubrication regime. In other words, the damaged gear was real, but it was also a symptom of a train-level issue.

The plant now faced a familiar problem. OEM replacement would restore the nominal design, but the delivery window was commercially difficult for the operation. An alternative path was evaluated based on full geometry capture, material verification, manufacturing qualification, and a parallel plan to correct alignment behavior during installation. The result was not simply a faster replacement part. It was a controlled recovery package: reproduce the gear to the required standard, verify the support system, restore lubricant delivery, and commission with early inspection points. The important lesson was that the best outcome did not come from choosing between OEM and non-OEM in abstract terms. It came from combining correct manufacturing with a correct understanding of why the first gear became distressed.

Conclusion

In heavy industry, gear damage should rarely be treated as an isolated component problem. What appears on the tooth flank is often only the visible result of a broader system condition shaped by alignment, load distribution, lubrication behavior, structural rigidity, and operating practice. For that reason, the most effective response is not simply to replace the failed part, but to understand why the damage developed, how the surrounding system contributed to it, and what risks remain if the same conditions are left unchanged.

The same logic applies to replacement strategy. OEM supply may remain the preferred path in some cases, but long lead times and operational pressure often require a more flexible and technically disciplined alternative. When reverse engineering, material verification, process control, and inspection are handled correctly, non-OEM replacement can provide a reliable and practical solution without compromising performance.

Ultimately, the strongest engineering decisions come from combining failure understanding with supply strategy. Plants that evaluate gears as part of a working system—rather than as isolated spare parts—are better positioned to reduce downtime, control risk, and recover faster when failures occur.

pamilanga.com

For Related Articles Search
failure analysis
at geartechnology.com

Engage to Stay Out in Front

Mary Ellen Doran, VP, Emerging Technology, MPMA

Mary Ellen Doran provides an update on emerging technology activities at the 2025 SNL.

Humanoid robots, eVTOL aircraft, and additive manufacturing at production scale. Each of these technologies will create real demand for precision gears and bearings, and real disruption for the manufacturers who supply them. The question is whether our industry helps shape that transition or reacts to it afterward.

MPMA's Emerging Technology committees exist to make sure it's the former. Here are four ways to be part of that work.

1. Join a Committee

MPMA runs five Emerging Technology committees: Robotics, Electric Vehicle Technology, IIoT, 3D Printing, and the newly formed Air Mobility Technology Committee. Each one meets regularly to discuss the technology through the lens of the gear and bearing manufacturer. As a committee we track developments, vet speakers for MPMA events, bring in expertise for informed discussions, host live events, and produce white papers that put the conversation on the record.

What you get out of a committee isn't just information—it's access to a different kind of peer group. The engineers and technical specialists who show up are thinking seriously about where the industry is heading, asking questions that don't have clean answers yet, and willing to work through them out loud. The Robotics Committee, for example, has drawn component designers, gearbox manufacturers, and systems integrators, all looking at the same technology from different vantage points. The conversation that comes out of a room like that is more useful than anything a single presenter could deliver, because it reflects the actual complexity of bringing a new technology into production.

If your professional network is deep in one area but narrow across disciplines, the committees are a practical way to change that.

2. Attend a Live Webinar

MPMA's live webinars bring in outside experts to give our audience an honest assessment of where a new technology stands—not the press release version. Recent sessions have featured Airwave's real-world application of AI in safety glasses and Liebherr's overview of their new SkiveFinishing process for internal gears.

The live format matters. You can ask questions, hear what your peers are wondering about, and get answers in real time. The presenters we invite are chosen from committee member input—they can separate signal from noise and they are candid about what is unknown.

3. Watch On-Demand Webinars

Not every schedule allows for a live session, and sometimes the most useful webinar is one you missed six months ago. Every MPMA Emerging Technology webinar is recorded and available for free on demand on the MPMA website, spanning topics from cybersecurity frameworks affecting manufacturers to new gearbox innovations entering production.

If you are new to a topic, the on-demand library is a practical place to start. An hour with the right presenter can do more to calibrate your thinking than a year of reading headlines.

4. Meet Emerging Tech Speakers at the MPMA SNL and FTM

The Strategic Networking & Leadership Forum (SNL) is where these conversations get personal—a smaller, more focused setting than the MPT Expo, designed for the kind of back-of-the-room discussions that don't happen on a conference stage. Some of the most valuable insights from our program have come not from presenters but from the conversations those presenters started.

This year, for the first time, the Fall Technical Meeting (FTM) will have a second concurrent track focused on emerging technologies, innovative solutions, and real-world applications. Join us in October.

Join the Conversation

None of this works without people willing to engage, show up, ask hard questions, and share what they know from the floor of real manufacturing operations. If that sounds like you, please join us, or reach out to me directly at *doran@motionpower.org*.

New Document Addresses the Challenges of EV Drivetrains

Todd Praneis, VP, MPMA Technical Division

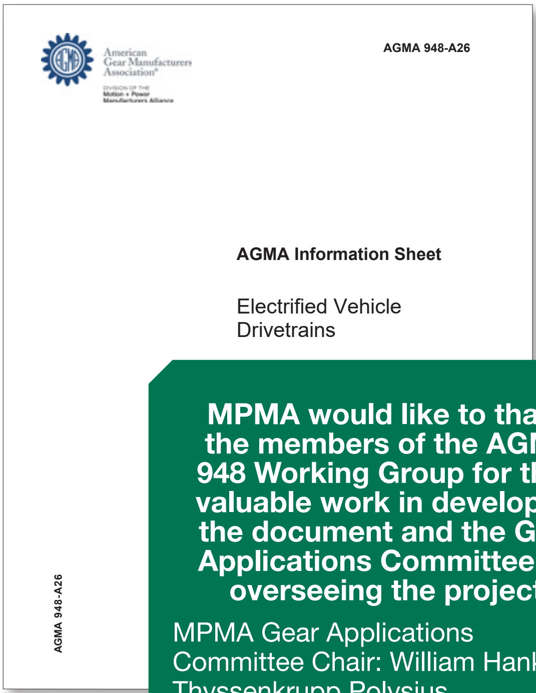
American Gear Manufacturers Association® Division of the Motion + Power Manufacturers Alliance

AGMA 948-A26

AGMA Information Sheet

Electrified Vehicle Drivetrains

AGMA 948-A26

The Motion + Power Manufacturers Alliance (MPMA) has released AGMA 948-A26, *Electrified Vehicle Drivetrains,* a comprehensive design guidance document for engineers developing geartrains and mechanical systems for hybrid, battery-electric, and plug-in hybrid electric vehicles. Approved by the MPMA Board of Directors on April 23, 2026, it marks a significant milestone as the industry navigates one of the most consequential transitions in vehicle engineering.

Why This Document Was Needed

Electrified powertrains impose fundamentally different requirements on mechanical components. Electric motors operate at higher speeds with sharper torque transients. Regenerative braking introduces bi-directional loading. Near-silent operation raises the bar for NVH performance, as gear whine previously masked by engine noise becomes clearly audible. High-voltage systems also introduce concerns around bearing current damage, electromagnetic compatibility, and lubricant chemistry.

The industry identified this gap in May 2021, when the AGMA Electric Drive Emerging Technology Committee published the white paper *A Gearing Centric Snapshot of the EV Space*. A working group convened in Detroit in June 2024, and the project was approved by the AGMA Technical Division Executive Committee in October 2024.

What the Document Covers

AGMA 948-A26 addresses design considerations for electrified drivetrains across ground and marine applications, including passenger cars, commercial vehicles, construction and agricultural equipment, mining vehicles, and watercraft. Topics include:

Duty cycle and loading—drive cycle definition, high-cycle survivability, inertial loading, and reverse loading during regenerative braking. Drivetrain configuration—inline, offset, planetary, parallel-axis, overhung, and wheel hub motor architectures, plus housing deflection limits, park lock design, and differential integration. NVH performance—damping strategies, motor excitation, torque ripple, and motor controller feedback. Gear design—electrical harmonics through tooth count selection, high contact ratio gearing, profile and lead modifications, surface finishing, transmission error analysis, and ripple/waviness measurement. Bearings, seals, and lubrication—electrical insulation, shaft current mitigation, high-speed lubrication, viscosity and efficiency trade-offs, and thermal management. Manufacturability and maintenance, including high-voltage safety considerations.

AGMA 948-A26 is available at *motionpower.org*.

MPMA would like to thank the members of the AGMA 948 Working Group for their valuable work in developing the document and the Gear Applications Committee for overseeing the project.

MPMA Gear Applications Committee Chair: William Hankes, Thyssenkrupp Polysius

MPMA Gear Applications Committee Vice Chair: Walt Weber, Flender Corporation

AGMA 948 Project Leader: John O'Neil, Star SU, LLC

Contributors

Anu Anisetti, Eaton Corporation

Michael Tekletsion Berhan, Ford Motor Company

Matthew Bollman, Charter Steel

Jeffrey Daniels, Twin Disc, Incorporated

Jacob Dickie, Ontario Drive & Gear Ltd.

Brett Dionne: RENK Group

Vanyo Kirov, Caterpillar

Michael McKernin, Croix Gear

Jitesh Modi, Schaeffler

Calogero Principato, KISSsoft AG

Andy Raycraft, JTEKT North America

Ernie Reiter, Web Gear Services Ltd.

Brian Rhode, Afton Chemical Corporation

Patrick Ridgley, The Boeing Company

J. Kirk Storey, Alchemetric Engineering, LLC

David Talbot, Ohio State University, Dept. of Mechanical Engineering

Antoine Türich, Gleason Corporation

Dairene Uy, Shell Global Solutions (US) Inc.

Allen Williston, A & J Engineering

Carlos Wink, Eaton Corporation

Hai Xu, General Motors LLC

Shuo Zhang, Allison Transmission, Inc.

Analytical Calculation of the Gear Body Stiffness of Face Gears

Jonas-Frederick Berger (b. Hochrein), Dr.-Ing. Michael Otto and Dr.-Ing. Karsten Stahl

Introduction and Motivation

The requirements for gearboxes are constantly growing. Among other factors, driven by the concept of achieving sustainability (Ref. 1) and the increasing requirements of e-Mobility, gearboxes are being designed increasingly for maximum performance. The load distribution in the gear contact is a fundamental quantity in the design phase, which is used to design micro-modifications and to determine lifetime. The load distribution can be calculated numerically with full-contact finite element analysis (FE) or with (semi-) analytical methods. Full FE contact investigations are complex and time-consuming. The tooth contact simulation of a gearbox can easily take several hours or even days. This is the reason why alternative methods have been developed and are worthy of further research. Methods deviating from the full FE contact analysis are often summarized in the literature under the term *loaded tooth contact analysis* (LTCA). With these, analyses are often possible within seconds to a few minutes. In LTCA, stiffnesses of the gear components (housing, bearings, shafts, gearing, etc.) are determined and assembled in a global system stiffness matrix (Refs. 2–6). Tooth stiffness is an essential component in LTCA. Typically, the tooth stiffness is divided into three parts as shown in Figure 1: a) Tooth deformation (normal, shear, and bending deformation); b) Gear body deformation (Tooth tilting deformation); and c) Contact deformation.

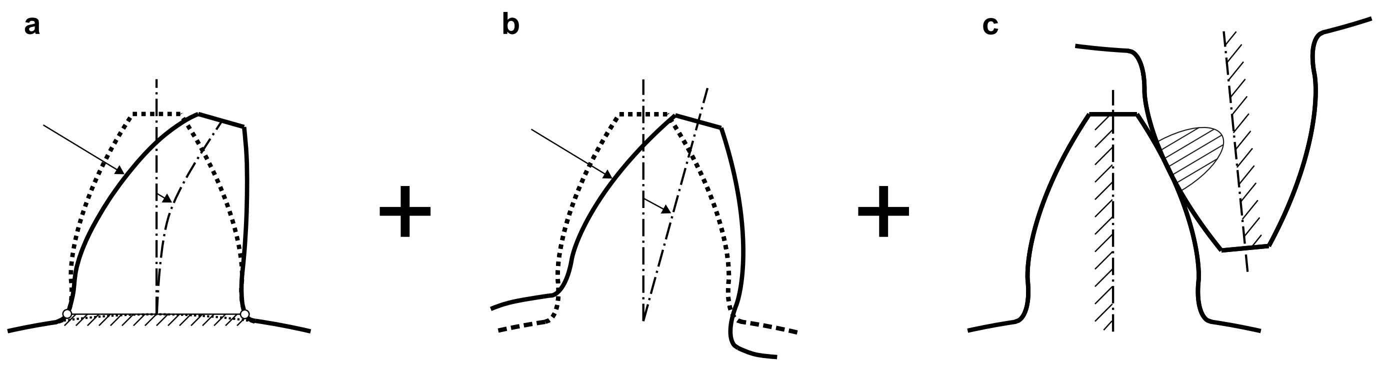

Figure 1—Components of tooth deformation (stiffness) according to Weber and Banaschek (Ref. 7): a) Tooth bending deformation with clamped tooth root; b) Tooth tilting deformation with stiff tooth (gear body deformation); and c) Contact point deformation.

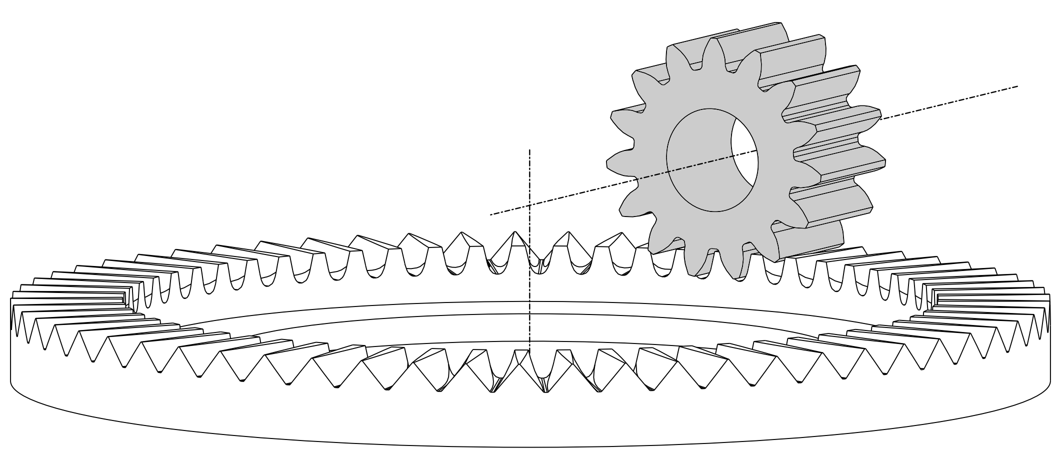

Figure 2—Exemplary face gear drive. Pinion in gray and face gear in white. Reprinted from Ref. 8.

A comprehensive review of analytical, hybrid and pure FE methods for tooth stiffness calculation is provided by Marafona et al. (Ref. 9) and Natali et al. (Ref. 10). A basic method for calculating gear body stiffness analytically goes back to Weber and Banaschek (W/B) from 1953 (W/B) (Ref. 7). The theory is widely used (Refs. 9,11–14) and even found its way in standards indirectly through the series development of the tooth stiffness (Refs. 15–17). For the gear body deformation/stiffness, W/B assumes that the tooth is rigid and that the connecting parts of the gear body deform elastically when force is applied. Figure 3a shows the applied contact force P on the tooth at the contact point.

The projection onto the tooth centerline yields the height y_{p} above the tooth root. The moment/force components on the wheel body, therefore, decompose to:

$$M = P\cos(\alpha')\,y_{\mathrm{p}} \tag{1}$$

$$Q = F_{\mathrm{s}} = P\cos(\alpha') \tag{2}$$

$$N = F_{\mathrm{d}} = P\sin(\alpha') \tag{3}$$

The gear body is represented as a half-plane on which boundary stresses/line loads along the tooth root thickness b are specified. Even though the tooth is stiff, the base surface where the line loads are applied can deform freely. The boundary stresses are intended to reproduce the stress state at the tooth root. Figure 3 shows the boundary loads for bending (b), normal (c), and shear load (d). The loads in Figure 3b–d are used to determine the deformation of the half-plane and the partial work integrals. Summing up and equating the partial work integrals with the work done by the external load P results in the deformation u_{WB} in the direction of engagement. Finally, after extensive analytical solving of the partial work integrals, W/B gives an equation for u_{WB} that is valid for v=0.3:

The analytical-mechanical approach according to Weber and Banaschek (Ref. 7) shows good agreement with experimental investigations (Refs. 19–23).

Face gear drives are a special type of angular gear unit, in which an involute pinion meshes with a face gear wheel (Refs. 24, 25). The pairing can be helical and with or without center offset. Figure 2 shows an exemplary spur face gear drive configuration without center offset. The pressure angle of the face gear wheel is variable across the tooth width and increases towards the outside radius (Refs. 26, 27). One advantage of face gear drives is that both gearings can be manufactured on conventional cylindrical gear machines, and the contact pattern in the axial direction of the pinion does not need to be adjusted (Ref. 25).

However, the comparison of the gear geometries in Figure 2 leads to the conclusion that the approaches for calculating the gear body stiffness of cylindrical gears cannot represent the deformation state of face gear wheels. Due to the plane shape of the face gear wheel, it is to be expected that the deformation increases in the direction of the outer radius. As a result, the stiffness of the gear body decreases toward the outer radius. This work aims to develop a basic model for calculating the gear body stiffness of face gear wheels based on mechanical analytical approaches.

This article is an abridged version of the presentation of the same name given at the AGMA Fall Technical Meeting 2024 (Ref. 28). For more in-depth information, please refer to the corresponding article.

Development of a Calculation Method for the Gear Body Stiffness of Face Gears

The method developed in this work for calculating the gear body stiffness of face gear wheels works analogously to the method according to W/B. However, plate and disk formulations are used for the calculation to accurately represent the deformation states of the face gear wheel. The cylindrical mechanical plate formulation serves to determine the deforma-

$$u_{\mathrm{WB}} = \frac{P}{EL}\cos^2(\alpha')\left(5.2\frac{y_{\mathrm{p}}^2}{b^2} + \frac{y_{\mathrm{p}}}{b} + 1.4\left(1 + 0.294\tan^2(\alpha')\right)\right) \tag{4}$$

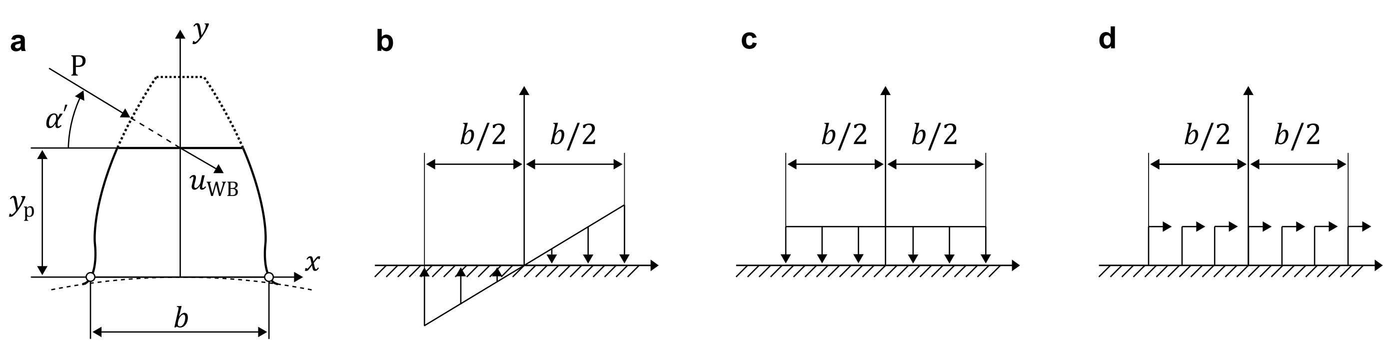

Figure 3–Model for determining gear body deformation (stiffness) in the direction of engagement according to Weber and Banaschek (Ref. 7): a) Vector decomposition of the contact force P; b) Linear line load (normal) for representation of the bending moment M ; c) Constant line load (normal) for representation of the pressure force N ; d) Constant line load (shear) for representation of the shear force Q . (Figures adapted from Ref. 18; l = Tooth width.)

tion components perpendicular to the wheel center plane (see the "Out-of-Plane Solution" section). The cylindrical mechanical disk formulation serves to determine the deformation components within the wheel center plane (see the "In-Plane Solution" section). The wheel body is modeled as a flat circular plate/disk with constant thickness. Figure 4a shows the coordinate system and structure of the plate and disk models used in this work. As the face gear wheel is circular, a polar coordinate system (r,θ,z) is appropriate. r_o and r_h are the outer and hub radii of the face gear wheel. The calculation is performed by specifying various line loads along an arc segment from $-\varepsilon$ to ε at a radius r_f between the hub and outer radius. To solve the deformation states, the plate/disk must be divided into two areas. The first area (I) extends from the hub radius r_h to the radius r_f at which the load is specified. The second area (II) extends from r_f to the outer radius r_o. While Figure 4b–c shows the load specification for the plate (out-of-plane), Figure 4d–e shows the load specification for the disk model (in-plane).

Out-of-Plane Solution

The load cases, normal and bending deformation (Figure 3b–c) according to W/B, are also applied in the plate model. This work uses the Kirchhoff-Love theory. The deformation w in z-direction of a circular plate perpendicular to its middle plane (x-y plane in Figure 4) follows the equation (Refs. 29–31):

$$\Delta\Delta w(r,\theta) = \frac{q(r,\theta)}{K} \tag{5}$$

q is the surface load on the plate, which does not exist in the model used in this work. Therefore $q(r,\theta)=0$. K is the plate bending stiffness (Refs. 29–31):

$$K = \frac{Eh^3}{12(1-v^2)} \tag{6}$$

Δ is the La-Place Operator in polar coordinates (Refs. 29–31):

$$\Delta \frac{\partial^2}{\partial r^2} + \frac{1}{r}\frac{\partial}{\partial r} + \frac{1}{r^2}\frac{\partial^2}{\partial \theta^2} \tag{7}$$

The constitutive equations for the internal forces and moments, as well as the kinematic relations, can be obtained from standard mechanical works (Refs. 29–32). The solution of the biharmonic function $\Delta\Delta w=0$ can be achieved with the series expansion of the deformation (Refs. 32, 33):

$$w = R_0 + \sum_{n=1}^{j} R_n \cos(n\theta) + \sum_{n=1}^{j} R'_n \sin(n\theta) \tag{8}$$

The series is terminated after j terms. Amongst others, the elementary functions R_0, R_n and R'_n are specified in Refs. 31–36. For the plate deformation, boundary conditions (BC) at the hub and outer radius, and transition conditions (TC) between the plate areas I and II at r_f are necessary. These are (Ref. 37):

- Fixed clamping at hub radius: Deformation and its first derivative (slope) equal zero (2 BC)
- Free end at outer radius: Shear force and moment equal to zero (2 BC)
- Continuity at the transition between areas I and II: Displacement and first (slope) and second derivative (curvature) of the displacement are equal (3 TC)
- Balance of forces at the transition between areas I and II with the external loading (1 TC)

All in all, this results in a total of eight conditions that are sufficient to solve the problem for different loads.

Normal Deformation: Constant Line Load from $-\varepsilon$ to ε

The normal deformation perpendicular to the gear body is determined with a constant line load (Figure 4b). The bihar-

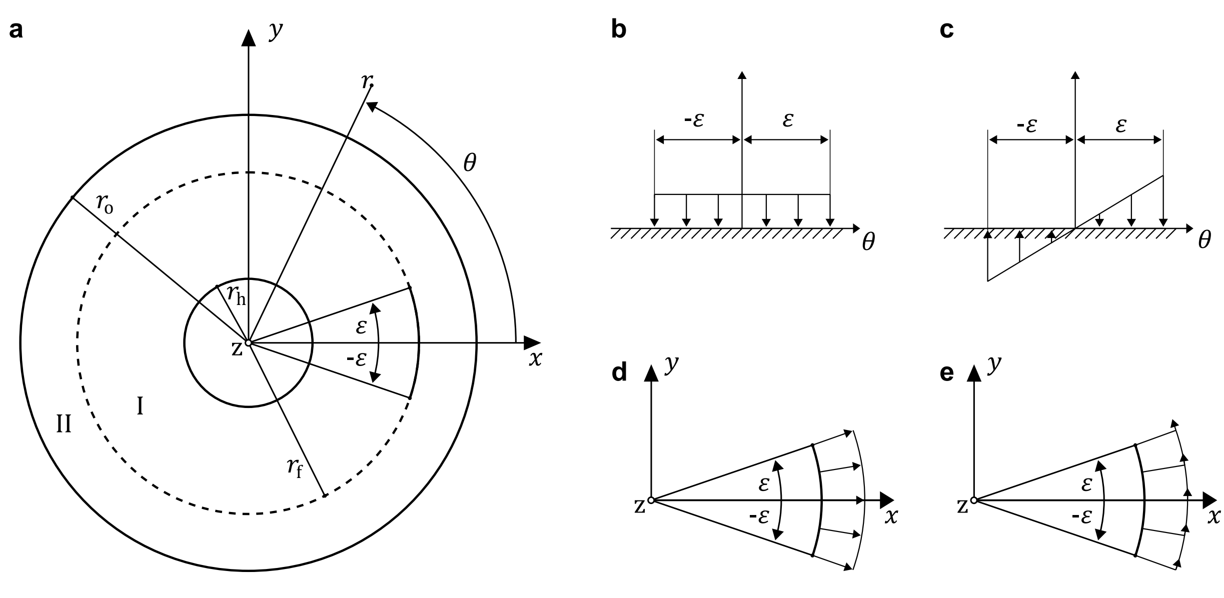

Figure 4—Model proposed in this work to determine the gear body deformation (stiffness) of face gears: a) Coordinate system and structure of the plate/disk model; b) Constant line load in the z-direction (out-of-plane) of the plate; c) Linear line load in the z-direction of the plate; d) Constant radial line load in the r-direction of the disk; and e) Constant tangential line load in the circumferential direction of the disk.

monic function $\Delta\Delta w$=0 is solved using a trigonometric series expansion. Therefore, the constant line load must also be developed in a trigonometric series. The Fourier series expansion is suitable for this (Refs. 38, 39). The plate is loaded along the angle segment -ε to ε with a constant normal force F_d at the radius r_f. The constant line load thus results in:

$$p_d = \frac{F_d}{2\varepsilon r_f} \tag{9}$$

The Fourier series development of the constant line load p_d is (Ref. 39):

$$f_d = \frac{p_d \varepsilon}{\pi} + \sum_{n=1}^{j} \frac{2p_d \sin(n\varepsilon)}{\pi n} \cos(n\theta) \tag{10}$$

The Fourier series f_d can only be calculated with a finite number of terms j. Since the Fourier series represents an even function, it consists of only one constant term and j cos terms dependent on θ. Figure 5 shows an exemplary ideal line load p_d (red) and the corresponding Fourier series expansion (black) in a with j=10 elements and b with j=100 elements. As the number of series terms increases, the Fourier series expansion approaches the ideal constant line load. The upper and lower overshoots of the Fourier series at the step points of constant line load distribution are referred to as Gibbs phenomenon (Refs. 38, 40). These make up about 18 percent of half the step height (Ref. 38).

Since the Fourier series of the line load f_d does not contain any odd components, these are also omitted in the series approach for the plate deformation:

$$w = R_0 + \sum_{n=1}^{j} R_n \cos(n\theta) \tag{11}$$

Bandera and Strozzi (Ref. 34) solve the plate model with clamped inner and outer radii loaded at an arbitrary radius with a point force. Ciavatti et al. (Ref. 37) solve the plate model with a clamped inner radius and free outer radius loaded at any radius with a point load. With these publications and descriptions above, the transfer to the model used in this work is easily possible.

Bending Deformation: Linear Line Load from -ε to ε

The bending deformation perpendicular to the gear body is determined with a linear line load (Figure 4c). A bending moment M_b is specified for the calculation, analogous to W/B. In contrast to W/B, however, the lever arm is extended by half the plate thickness h since the plate is reduced to its middle plane within the plate model. This results in the moment:

$$M_b = P \cos(\alpha') \left(y_p + \frac{h}{2} \right) \tag{12}$$

The extreme values/end values of the linear line load are:

$$p_b = \frac{M_b}{\frac{1}{6}(2\varepsilon r_f)^2} \tag{13}$$

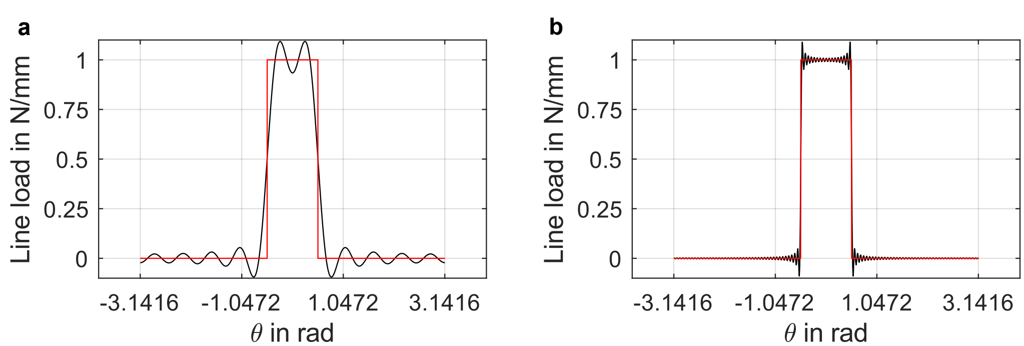

Figure 5—Fourier series expansion (black) of a constant line load (red); parametrization with* p_d *=1 and* $\varepsilon=\pi/6$*; and a) Fourier expansion with* j*=10 and b) Fourier expansion with* j*=100.

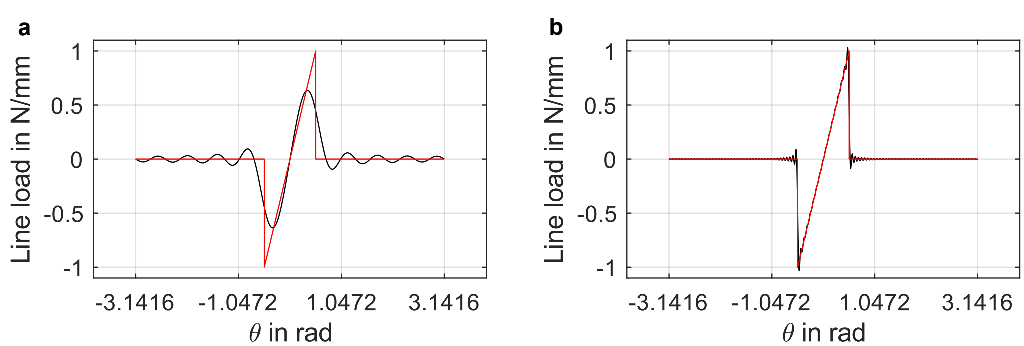

Figure 6—Fourier series expansion (black) of a linear line load (red); parametrization with* p_b *=1 and* $\varepsilon=\pi/6$*; and a) Fourier expansion with* j*=10 and b) Fourier expansion with* j*=100.

From the Fourier transformation follows the corresponding series expansion:

$$f_{\mathrm{b}} = \sum_{n=1}^{j} \frac{2p_b}{\varepsilon \pi n^2}(\sin(\varepsilon n) - \varepsilon n \cos(\varepsilon n))\sin(n\theta) \tag{14}$$

The linear line load is an odd function, which is why the Fourier series f_{b} only contains sin terms depending on θ (Ref. 38). Analogous to Figure 5, Figure 6 shows the linear line load (red) and the Fourier series representation (black). As with the constant line load, the ideal line load is more accurately represented as the number of series elements j increases.

Since the Fourier series of the line load f_{b} does not contain any even and constant components, these are also omitted in the series approach for the plate deformation:

$$w = \sum_{n=1}^{j} R_{\mathrm{n}}' \sin(n\theta) \tag{15}$$

The solution process for determining the missing constants from the boundary and transition conditions works in the same way as the load case with constant line load before.

In-Plane Solution

The plate model from the previous section is not suitable for the deformation components within the gear body plane. These can be determined using a disk model. For this, the stress function ϕ must also fulfill the biharmonic equation (Refs. 29, 30, 41, 42):

$$\Delta\Delta\phi(r,\theta) = 0 \tag{16}$$

The generally valid form of the stress function in polar coordinates can be found in standard mechanical literature (Refs. 41, 42). The stress components in the disk follow from the stress function (Ref. 41):

$$\sigma_{\mathrm{r}} = \frac{1}{r}\frac{\partial \phi}{\partial r} + \frac{1}{r^2}\frac{\partial^3 \phi}{\partial \theta^2} \tag{17}$$

$$\sigma_{\theta} = \frac{\partial^2 \phi}{\partial r^2} \tag{18}$$

$$\tau_{\mathrm{r}\theta} = \frac{1}{r^2}\frac{\partial \phi}{\partial \theta} - \frac{1}{r}\frac{\partial^2 \phi}{\partial r \partial \theta} = -\frac{\partial}{\partial r}\left(\frac{1}{r}\frac{\partial \phi}{\partial \theta}\right) \tag{19}$$

The stress-strain (displacement) relations are given in the literature (Refs. 41, 43–46). The following boundary and transition conditions are sufficient for solving the disk deformation in radial (u) and circumferential (v) directions:

- Fixed clamping at hub radius: Deformation in radial (u) and circumferential (v) directions equal zero (2 BC)
- Free end at outer radius: Stresses equal to zero (2 BC)
- Continuity at the transition between areas I and II: Deformation in radial (u) and circumferential (v) directions are equal (2 TC)
- Balance of stresses at the transition between areas I and II in radial (u) and circumferential (v) direction with the external loading (2 TC)

Radial Deformation: Radial Constant Line Load from -ε to ε

In the calculation of the partial deformations according to W/B for cylindrical wheel bodies, the tooth can be loaded in the normal section. The three stresses in Figure 3b–d are therefore sufficient to represent the stress state at the tooth root. The plate and disk models used in this paper can be solved for loading along an angular segment from -ε to ε of constant radius r_{f}, which corresponds to the transverse section cylinder at a face gear wheel. External loading in the normal section plane at the face gear wheel is not straightforward with plate and disk models. In contrast to W/B, a fourth stress component is therefore included in the model to represent the influence of axial force at the contact point (Figure 4d). Analogous to the constant normal line load from "Normal Deformation" section, the constant radial line load follows to:

$$p_{\mathrm{r}} = \frac{F_{\mathrm{r}}}{2\varepsilon r_{\mathrm{f}}} \tag{20}$$

For the disk model the Fourier series expansion of the external loading must also be developed into a boundary stress condition. The boundary stress is obtained by dividing the line load p_r by the disk thickness:

$$\sigma_{\mathrm{r}} = \frac{p_{\mathrm{r}}\varepsilon}{\pi h} + \sum_{n=1}^{j} \frac{2p_{\mathrm{r}}\sin(n\varepsilon)}{\pi h n}\cos(n\theta) \tag{21}$$

The Fourier series development of the boundary stress is not shown graphically here, as this is analogous to Figure 5. The solution of the disk equations and the determination of the deformations in radial (u) and circumferential (v) direction were developed and described in detail by DuBois (Ref. 47) for a circular disk with radial point load at the outer radius. Furthermore, Serati et al. (Ref. 45) describe the solution for a radially loaded disk. With these and with the description of the BCs and TCs from the "In-Plane Solution" section, the transfer of the solution method for the disk model with areas I and II as well as a distributed constant line load is possible without any problems.

Shear Deformation: Circumferential Constant Line Load from -ε to ε

The shear deformation of the gear body is modeled with a constant shear load at the disk (Figure 4e), analogous to W/B. As with the previous line loads, the constant shear line load along the load path from -ε to ε is:

$$p_{\mathrm{s}} = \frac{F_{\mathrm{s}}}{2\varepsilon r_{\mathrm{f}}} \tag{22}$$

The Fourier series expansion of the shear stress is therefore:

$$\tau_{\mathrm{r}\theta} = \frac{p_{\mathrm{s}}\varepsilon}{\pi h} + \sum_{n=1}^{j} \frac{2p_{\mathrm{s}}\sin(n\varepsilon)}{\pi h n}\cos(n\theta) \tag{23}$$

The deformation is solved analogously to the radial load. Srinivasan and Ramamurti (Ref. 48) describe the solution of a disk with concentrated edge load on the outer radius.

Face Gear Wheel Body Stiffness Calculation

The deformation in the direction of engagement u_{PD} at a radius r_{f} can be determined by balancing the partial work integrals w (Refs. 7, 49) done by the external line loads at the plate/disk against the work from the external force P:

$$\frac{1}{2}Pu_{\mathrm{PD}} = w_{\mathrm{d}} + w_{\mathrm{b}} + w_{\mathrm{s}} + w_{\mathrm{r}} \tag{24}$$

The partial work integrals are determined from the respective external ideal line loads p and deformations w along the load paths Γ:

$$w = \frac{1}{2}\int_{\Gamma} pwd\Gamma \tag{25}$$

Herein u_{PD} is u_{WB} in Figure 3a for the plate/disk approach. The deformation solutions for normal (d), bending (b), shear (s), and radial load (r) are known from the previous sections. At the contact point, the contact force P must be divided into its components (Figure 3a + the radial component out of the transverse section) and used to determine the partial deformations according to the "Out-of-Plane Solution" and "In-Plane Solutions" sections. The deformations are calculated along the load path from -ε to ε only and the work w resulting from this is determined using the respective ideal line load (red curves in Figure 5 and Figure 6). Determining the work integrals in this way has the advantage that the deformation only must be determined along the load path and not along the entire circumference of 2π. This means that considerably fewer points need to be calculated. The deformation in the direction of engagement and the contact force result in the gear body compliance q'_{R} or the wheel body stiffness c'_{R}:

$$q'_{\mathrm{R}} = \frac{u_{PD}}{P} \rightarrow c'_{\mathrm{R}} = {q'_{R}}^{-1} \tag{26}$$

Typically, P=1 N is used to obtain the compliance directly. However, due to the linear elasticity theory, any other force P can also be specified.

Results

Table 1 shows the face gear drive parameters used for the following validations. The data has already been used for other investigations on face gear drives (Refs. 18, 50). The macro tooth geometry is shown in Figure 2. The half angle ε results from the number of teeth z of the face gear wheel. The load path from -ε to ε extends over the angular pitch τ:

$$\varepsilon = \frac{1}{2}\tau = \frac{1}{2}\left(\frac{2\pi}{z}\right) \tag{27}$$

The validation of the methods described for calculating plate and disc deformation using the Fourier series approach is included in the conference paper (Ref. 28). In addition, the corresponding conference paper contains an analysis of the influence of the Fourier series parameter j on the convergence of the partial work integrals.

The aim is to develop a method for gear body stiffness for face gear wheels. Using the method from the "Face Gear Wheel Body Stiffness Calculation" section, this is possible along the tooth width (face gear radius). For the calculation, it is necessary to split the force P at the contact point into the individual force components (normal, bending, shear, and radial). Usually, the force components and directions (pressure angle) result from a load-free tooth contact simulation. For spur face gear drives (β=0), the pressure angle can also be approached from the model of the curved gear rack (Refs. 26, 27):

$$\cos(\alpha') = \frac{m_{\mathrm{n}} z \cos(\alpha_{\mathrm{n}})}{2r} \tag{28}$$

Herein, m_{n} is the normal module, z is the face gear teeth number, and α_{n} is the normal pressure angle of the pinion/cutter. The relationship thus gives the face gear pressure angle along the tooth width (radius r). The force/moment components result from the equations according to W/B in the "Introduction and Motivation" section. The radial force component is zero for spur face gears (Ref. 51). The W/B approach

Parameter	Symbol	Value	Unit
Face gear teeth number	z	61	-
Face gear hub radius	r_{h}	12.5	mm
Face gear inner radius of the teeth	r_{i}	29.5	mm
Face gear outer radius of the teeth	r_{o}	37.6	mm
Face gear thickness below the teeth	h	6	mm
Normal module	m_{n}	1	mm
Pinion normal pressure angle	α_{n}	20	°
Modulus of elasticity	E	210000	MPa
Poisson ratio	ν	0.3	-

Table 1—Design parameters of the exemplary spur face gear from Figure 2.

is essentially a 2D model of a plane with different loads on the boundary. To determine the stiffness across the tooth width with variable pressure angle, the gear tooth is divided into single slices (thin-slice model). With the previous equation, it is obvious that the pressure angle α' increases over the face gear tooth width. W/B applied to each single slice results in the gear body stiffness curve in Figure 7. The stiffness curve shows almost linear behavior. Due to the slice model, the stiffness is related to the slice thickness and given per unit face width. The unit N/(mm*µm) is chosen according to ISO 6336 (Ref. 16). The stiffness for the slice model is normalized to the slice thickness, as it changes with the thickness. Due to normalization, the curve in Figure 7 is independent of the number of slices (slice thickness). Figure 7 clearly shows that—when the method according to W/B is applied directly—the gear body stiffness increases along the tooth width. The deviation of the stiffness between the outer and inner radius for the W/B approach is:

$$\frac{c_{\mathrm{R}}'(r_0)}{c_{\mathrm{R}}'(r_{\mathrm{i}})} - 1 = 0.64 \tag{29}$$

Figure 8 shows the gear body stiffness curve along the tooth width, determined using the method proposed in this work. Since the plate/disk approach is no longer a thin-slice model and the gear body stiffness is determined on the full model for discrete radii between the inner and outer radius of the teeth, the stiffness cannot be normalized to the slice thickness. This results in the unit N/µm. A qualitative comparison with the W/B method is therefore possible. In contrast to the W/B method in Figure 7, the gear body stiffness curve in Figure 8 shows a decreasing behavior. It is also evident that the curve does not show linear growth. The deviation of the stiffness between the outer and inner radius for the plate/disk approach is:

$$\frac{c_{\mathrm{R}}'(r_0)}{c_{\mathrm{R}}'(r_{\mathrm{i}})} - 1 = -0.81 \tag{30}$$

Discussion

The cylindrical plate and disk models with constant thickness approximate the real geometry of the face gear wheel. In reality, the gear bodies can be more complex in shape or can have a non-constant thickness along the radius. Especially at the hub, the thickness may be higher. However, particularly concerning the W/B method in the "Introduction and Motivation" section, in which the gear body of cylindrical gears is approximated as an infinite half-plane, the assumption of a circular plate/disk with constant thickness seems justified.

One advantage of the analytical formulation is that deformations can be calculated independently of any mesh

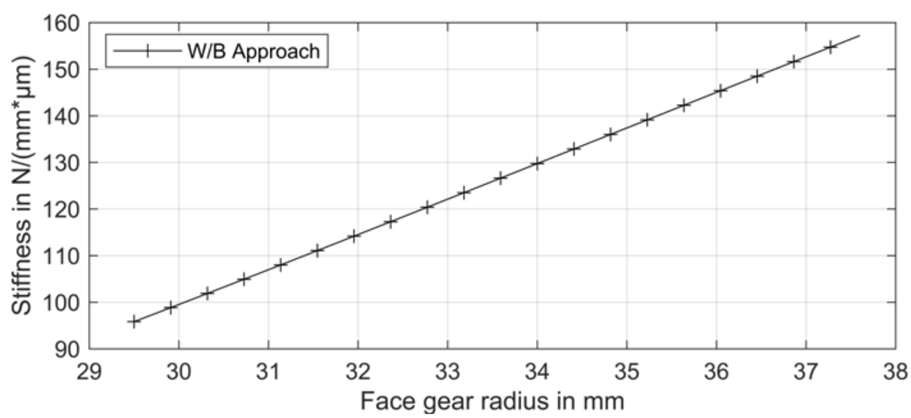

Figure 7—Gear body Stiffness along the face gear radius (tooth width), derived using the W/B method in single slices (y_p =1 mm). Tooth root width for W/B $b=2\varepsilon r_f$.

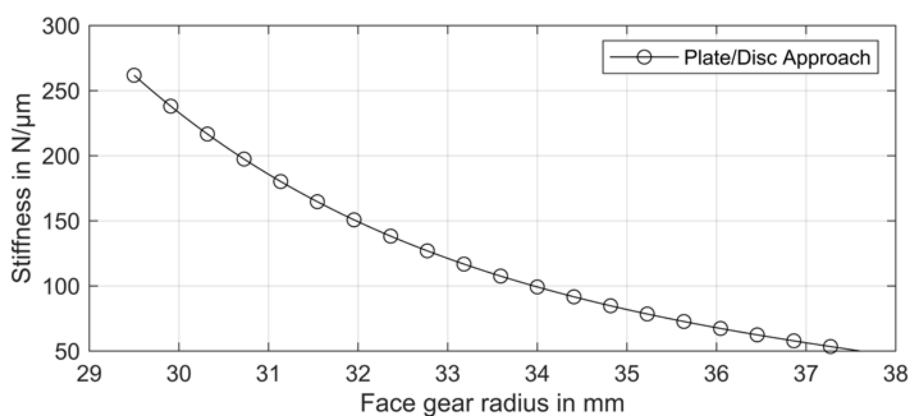

Figure 8—Gear body Stiffness along the face gear radius (tooth width), derived using the proposed method in this work (y_p =1 mm).

discretization. For work integrals, only the deformations along the load paths are relevant and need to be determined beforehand. This is possible with the analytical models. With FE methods, on the other hand, complete models must be solved. To apply the loads and reliably calculate the deformations, meshing must be appropriately fine around the loads in the FE method. Modeling and calculation time with the FE method is therefore significantly higher compared to the analytical approach. The analytical method mainly requires one-off work in developing the deformation equations.

The work integrals from the analytical deformation calculations yield the gear body stiffness at the contact point. In contrast to the developed method (Figure 8), the gear body stiffness increases along the tooth width for the conventional approach with the infinite half-plane in Figure 7. However, it must be noted that this approach was never developed for face gear wheels, but for cylindrical gears (Ref. 7). It just makes sense to use existing, established methods as a first try. One explanation for the increase in stiffness could be the deformation component of the normal force. With increasing radius, the face gear pressure angle α' and therefore the normal force increases. In the conventional approach, the work integral of the normal force (Figure 3c) is determined through a comparison approach (Ref. 7). In addition, it is already mentioned in the work that the influence of the normal force component will be subordinate (Ref. 7). This is certainly an appropriate assumption for cylindrical gears where the full material gear body is supported by a shaft at the hub but does not apply to face gear wheels. Due to the greater leverage with a larger radius, gear body stiffness should decrease along the tooth width. With the investigation in the "Results" section, it is obvious that the developed approach in this work shows the intended gear body stiffness behavior of face gear wheels (Figure 8).

The aim is to first develop a model to determine the face gear body stiffness. For validation, the calculation at one point in the profile direction for several slices in width was chosen, as the main change in stiffness is expected in the width. Nevertheless, the approach can also be used to determine stiffness in profile direction (time-dependent or as a function of the roll angle). For this purpose, the parameters y_P and α' must be chosen accordingly. These usually result from a load-free tooth contact analysis, which is not part of this work.

The calculation is based on an analytical material model. Non-linear behavior (e.g., for plastic) cannot be calculated directly. The analytical derivation is already complex, which would be enormously increased by using non-linear material behavior. Nevertheless, plastics can be represented in good approximation using adapted material parameters (modulus of elasticity and Poisson's ratio).

The load cases are not coupled in the analytical models. The in-plane and out-of-plane solutions are derived separately. This is certainly an assumption that must be made to enable analytical calculation. Analytical models for calculating the coupled loading/deformation are—to the best of the authors' knowledge—not available. The focus of this work is on fast analytical calculation. Coupled loading is possible with numerical models, but this increases the complexity and calculation time. However, the uncoupled analytical approach shows the expected behavior.

Conclusion and Outlook

Face gear drives are angular gear units, in which an involute pinion meshes with a face gear wheel. While the pinion is a cylindrical gear, the face gear wheel is disk-shaped. Conventional approaches for calculating gear body stiffness focus on cylindrical gears. The most accurate stiffness calculation is a prerequisite for the LTCA—apart from the full FE contact calculation—to determine valid results. This paper presents an analytical method for the gear body stiffness of face gear wheels based on an established approach in the "Development of a Calculation Method for the Gear Body Stiffness of Face Gears" section. The face gear wheel serves as a demonstration object. However, the approach can be directly transferred to other plate-shaped gears without great effort. The "Results" section confirms the developed model.

Different points can be mentioned as an outlook. The Kirchhoff-Love plate theory is applied to the out-of-plane deformation. An extension of the proposed method could be the use of a more advanced plate model, which takes shear deformation into account (Ref. 52). Higher-order plate formulations, such as the Reissner model, are described with a system of differential equations (Ref. 29). This makes the solution process much more complex, which is why the Kirchhoff-Love model was used in this work at first.

A further development of the proposed approach could be the incorporation of the stiffening effects of the gear teeth or the hub. Since the analytical plate/disk model in its current development stage only allows for constant thickness, FE-reference calculations could be used to derive a stiffness factor along the tooth width for various complex gear body shapes.

The paper developed and validated the basic approach for the gear body stiffness of disk-shaped gears. Further work will focus on the LTCA of face gear drives. The stiffness in the profile and width direction will be determined using the presented approach. It is expected that the load distribution over the flanks in meshing will change accordingly. One central aspect is the conversion of the plate/disk gear body stiffness formulation to a slice stiffness formulation, as used in LTCA.

Acknowledgements

The presented results are based on the research project AZ-1601-23 supported by the Bavarian Research Foundation (Bayerische Forschungsstiftung, BFS). The authors would like to thank for the sponsorship and support received from the BFS.

Jonas-Frederick Berger (b. Hochrein) earned his M.Sc. in Mechanical Engineering from the Technical University of Munich (TUM) in 2020. He is a PhD candidate and Team Leader for Gear Calculation Software at TUM's Gear Research Center (FZG), researching LTCA and gear geometry, especially for face gear drives and cylindrical gears.

Dr.-Ing. Michael Otto joined FZG in 2000 and has led the Calculation and Verification of Transmission Systems division since 2006. His research covers gear geometry, tooth contact analysis, NVH, and gearbox deformation and stress analysis. He also drives the development of scientific software available to FVA member companies.

Prof. Dr.-Ing. Karsten Stahl studied Mechanical Engineering at TUM, where he received his PhD at FZG. Since 2011, he is full professor and FZG director. His research focuses on endurance, tribology, NVH, and fatigue life in gearboxes and drive systems. He is president of the International Conference on Gears.

References

1. Anastas P. T., and Zimmerman J. B., 2003, "Design through the 12 principles of green engineering," *Environmental Science & Technology,* Vol. 37, No. 5, pp. 94A–101A. doi:10.1021/es032373g.
2. Neubauer B., Otto M., and Stahl K., 2015, "Efficient Calculation of Load Distribution and Design of Tooth Flank Modifications in Planetary Gear Systems: Static load and deformation analysis in a fully coupled mechanical model of a gear box structure with LAPLASn," International Conference on Gears 2015, VDI-Verl., Düsseldorf, pp. 549–558.
3. Weinberger U., Otto M., and Stahl K., 2020, "Closed-Form Calculation of Lead Flank Modification Proposal for Spur and Helical Gear Stages," *ASME. J. Mech. Des,* Vol. 142, No. 3. doi:10.1115/1.4045396.
4. Wu S.-H., and TSAI S.-J., 2009, "Contact stress analysis of skew conical involute gear drives in approximate line contact," *Mechanism and Machine Theory,* Vol. 44, No. 9, pp. 1658–1676. doi:10.1016/j.mechmachtheory.2009.01.010.
5. Placzek T., 1988, "Lastverteilung und Flankenkorrektur in gerad- und schrägverzahnten Stirnradstufen," Dissertation, Technische Universität München.
6. Winter H., and Placzek T., 1991, "Load Distribution and Topological Flank Modification of Helical and Double Helical Gears," *Eur. J. Mech. Eng.,* Vol. 36, No. 3, pp. 171–176.
7. Weber C., and Banaschek K., 1953. *Formänderung und Profilrücknahme bei gerad- und schrägverzahnten Rädern,* 1st ed., Friedrich Vieweg & Sohn, Braunschweig.
8. Hochrein J.-F., Otto M., and Stahl K., 2024, "Face gear drives: Nominal contact stress calculation for flank load carrying capacity evaluation," *Mechanism and Machine Theory,* Vol. 195. doi:10.1016/j.mechmachtheory.2024.105573.
9. Marafona J. D., Marques P. M., Martins R. C., and Seabra J. H., 2021, "Mesh stiffness models for cylindrical gears: A detailed review," *Mechanism and Machine Theory,* Vol. 166. doi:10.1016/j.mechmachtheory.2021.104472.
10. Natali C., Battarra M., Dalpiaz G., and Mucchi E., 2021, "A critical review on FE-based methods for mesh stiffness estimation in spur gears," *Mechanism and Machine Theory,* Vol. 161. doi:10.1016/j.mechmachtheory.2021.104319.
11. Spura C., and Berger G., 2011, "Ermittlung des Verformungs- und Steifigkeitsverhaltens von bombierten Profilwellenverbindungen mit Evolventenverzahnung," *Forsch Ingenieurwes,* Vol. 75, pp. 35–44. doi:10.1007/s10010-011-0132-9.
12. Spura C., 2015, "Berechnung der Verformungen und Steifigkeiten evolventischer Verzahnungen von Zahnkupplungen," *Forsch Ingenieurwes,* Vol. 79, pp. 5–15. doi:10.1007/s10010-015-0183-4.
13. Petersen D., 1989, "Auswirkungen der Lastverteilung auf die Zahnfußtragfähigkeit von hoch überdeckenden Stirnradpaarungen," Dissertation, Technische Universität Braunschweig.
14. *KISSsoft AG—A Gleason Company,* Ed., 2019. *KISSsoft Release 2019:* User manual.

15. Schäfer S., 1971, "Ein Beitrag zur Ermittlung des wirksamen Flankenrichtungsfehlers bei Stirnradgetrieben und der Lastverteilung bei Geradverzahnung," Dissertation, Technische Hochschule Darmstadt.
16. ISO 6336-1:2019-11, 2019, "Calculation of load capacity of spur and helical gears—Part 1: Basic principles, introduction and general influence factors."
17. DIN 3990-1:1987-12, 1987, "Tragfähigkeitsberechnung von Stirnrädern—Einführung und allgemeine Einflußfaktoren."
18. Hochrein J.-F., Otto M., and Stahl K., 2022, "Fast tooth deflection calculation method and its validation," *Forsch Ingenieurwes,* Vol. 86, pp. 845–859. doi:10.1007/s10010-022-00598-8.
19. Daffner M., 2018, "Validierung von Verformungsberechnungen im System Zahnrad-Welle-Lager-Gehäuse," Dissertation, Technische Universität München.
20. Winter H., and Podlesnik B., 1983, "Zahnfedersteifigkeit von Stirnradpaarungen Teil 1: Grundlagen und bisherige Untersuchungen," *Antriebstechnik,* Vol. 22, pp. 39–42.
21. Winter H., and Podlesnik B., 1983, "Zahnfedersteifigkeit von Stirnradpaarungen Teil 2: Einfluss von Verzahnungsdaten, Radkörpern, Linienlast und Wellen-Naben-Verbindung," *Antriebstechnik,* Vol. 22, pp. 51–58.
22. Winter H., and Podlesnik B., 1984, "Zahnfedersteifigkeit von Stirnradpaarungen Teil 3: Einfluss der Radkörperform auf die Verteilung der Einzelfedersteifigkeit und der Zahnkraft längs der Zahnbreite," *Antriebstechnik,* Vol. 23, pp. 43–49.
23. Daffner M., Otto M., and Stahl K., 2017, "Method of measuring the load distribution of spur gear stages," *JAMDSM,* Vol. 11, No. 6. doi:10.1299/jamdsm.2017jamdsm0076.
24. Litvin F. L., and Fuentes A., 2004. *Gear Geometry and Applied Theory,* 2nd ed., Cambridge University Press. doi:10.1017/CBO9780511547126.
25. Roth K., 1998. *Zahnradtechnik Evolventen-Sonderverzahnungen zur Getriebeverbesserung: Evoloid-, Komplement-, Keilschräg-, Konische-, Konus-, Kronenrad-, Torus-, Wälzkolbenverzahnungen, Zahnrad-Erzeugungsverfahren,* 1st ed., Springer Berlin, Heidelberg. doi:10.1007/978-3-642-58890-7.
26. Basstein G., and Sijtstra A., 1993, "Neue Entwicklungen bei Auslegung und Fertigung von Kronenrädern," *Antriebstechnik,* Vol. 32, No. 11, pp. 53–60.
27. Basstein G., and Sijtstra A., 1993. "New developments in Design, Manufacturing and Application of Cylkro-(Face) Gears," AGMA technical paper 93FTM7, American Gear Manufacturers Association, Alexandria, Virginia.
28. Berger J.-F., Otto M., and Stahl K., 2024. "Analytical Calculation of the Gear Body Stiffness of Face Gears," AGMA technical paper 24FTM08, American Gear Manufacturers Association, Alexandria, Virginia.
29. Altenbach H., Altenbach J., and Naumenko K., 2016. *Ebene Flächentragwerke: Grundlagen der Modellierung und Berechnung von Scheiben und Platten,* Springer Berlin Heidelberg, Berlin, Heidelberg. doi:10.1007/978-3-662-47230-9.
30. Girkmann K., 1963. *Flächentragwerke,* Springer Vienna, Vienna. doi:10.1007/978-3-7091-8096-9.
31. Föppl A., 1912, "Die Biegung einer kreisförmigen Platte," Sitzungsberichte der mathematisch-naturwissenschaftlichen Abteilung der Bayerischen Akademie der Wissenschaften zu München(II), pp. 155–190.
32. Timoschenko S. P., and Woinowsky-Krieger S., 1959. *Theory of Plates and Shells,* 2nd ed., McGraw-Hill, New York.
33. Reißner H., 1929, "Über die unsymmetrische Biegung dünner Kreisringplatten," *Ing. arch,* Vol. 1, pp. 72–83. doi:10.1007/BF02079709.
34. Bandera C., and Strozzi A., 1991, "Displacements in a clamped annular plate transversely loaded at an arbitrary point by a concentrated force," *International Journal of Pressure Vessels and Piping,* Vol. 49, No. 1, pp. 17–34. doi:10.1016/0308-0161(92)90070-V.
35. Strozzi A., 1989, "Mechanical analysis of an annular plate subject to a transverse concentrated load," *The Journal of Strain Analysis for Engineering Design,* Vol. 24, No. 3, pp. 139–149. doi:10.1243/03093247V243139.
36. Dragoni E., and Strozzi A., 1989, "Mechanical analysis of a simply supported annular plate loaded by a periphery force," *International Journal of Pressure Vessels and Piping,* Vol. 40, No. 3, pp. 175–191. doi:10.1016/0308-0161(89)90103-8.
37. Ciavatti V., Dragoni E., and Strozzi A., 1992, "Mechanical Analysis of an Annular Plate Transversely Loaded at an Arbitrary Point by a Concentrated Force," *Journal of Mechanical Design,* Vol. 114, No. 3, pp. 335–342. doi:10.1115/1.2926558.
38. Karpfinger C., 2022. *Calculus and Linear Algebra in Recipes,* Springer Berlin Heidelberg, Berlin, Heidelberg. doi:10.1007/978-3-662-65458-3.
39. Márkus G., 1985. *Kreis- und Kreisringplatten unter periodischer Belastung,* 1st ed., Werner, Düsseldorf.
40. Carslaw H. S., 1921. *Introduction to the Theory of Fourier's Series and Integrals and the Mathematical Theory of the Conduction of Heat*, 2nd ed., Macmillan, London.
41. Timoschenko S. P., and Goodier J. N., 1951. *Theory of Elasticity,* 2nd ed., McGraw-Hill, New York.
42. Michell J. H., 1899, "On the Direct Determination of Stress in an Elastic Solid, with application to the Theory of Plates," *Proceedings of the London Mathematical Society,* Vol. s1-31, No. 1, pp. 100–124. doi:10.1112/plms/s1-31.1.100.
43. Boresi A. P., Chong K. P., and Lee J. D., Eds., 2010. Elasticity in Engineering Mechanics, Wiley. doi:10.1002/9780470950005.
44. Sadd M. H., 2014. *Elasticity: Theory, Applications, and Numerics,* 3rd ed., Elsevier. doi:10.1016/C2012-0-06981-5.
45. Serati M., Alehossein H., and Williams D. J., 2012, "Elastic stress analysis of partially loaded hollow discs," *International Journal of Engineering Science,* Vol. 53, pp. 19–37. doi:10.1016/j.ijengsci.2011.12.010.
46. Biezeno C. B., and Grammel R., 1953. *Technische Dynamik,* 2nd ed., Springer Berlin Heidelberg, Berlin, Heidelberg. doi:10.1007/978-3-642-65187-8.
47. DuBois R. P., 1970, "Buckling loads of tensioned circular plates subject to concentrated in-plane loading," Master's thesis, Kansas State University, http://hdl.handle.net/2097/7439.
48. Srinivasan V., and Ramamurti V., 1980, "Stability and vibration of an annular plate with concentrated edge load," *Computers & Structures,* Vol. 12, No. 1, pp. 119–129. doi:10.1016/0045-7949(80)90100-5.
49. Weber C., 1947. *Festigkeitslehre,* Wolfenbütteler Verlags Anstalt, Wolfenbüttel-Hannover.
50. Hochrein J.-F., Güntner C., Otto M., and Stahl K., 2024, "Face gear drive manufacturing: Pinion/cutter design for a crowned contact pattern," *Proceedings of the Institution of Mechanical Engineers, Part B: Journal of Engineering Manufacture,* Vol. 238, No. 9, pp. 1282–1292. doi:10.1177/09544054231196597.
51. Tsai S.-J., 1997, "Vereinheitlichtes System evolventischer Zahnräder: Auslegung von Zylindrischen, Konischen, Kronen- und Torusrädern," Dissertation, Technische Universität Braunschweig.
52. Panc V., 1975. *Theories of Elastic Plates,* 1st ed., Noordhoff, Leyden.

Shortened from a longer paper first presented at the 2025 Fall Technical Meeting (FTM), October 22–24, 2025, Detroit, and printed with permission of the author(s). Statements presented in this paper are those of the author(s) and may not represent the position or opinion of the American Gear Manufacturers Association.

Klingelnberg

EXPANDS DIGITAL SOLUTIONS WITH NEW SMART TRACING

Under the umbrella of Aiktec–Digital Solutions, Klingelnberg brings together smart, industry-ready applications that bring the concepts of Industry 4.0 and the IoT directly to the shop floor.

Smart Tracing is a web-based software solution for analyzing machine behavior. It is essentially the Klingelnberg DDQM (Data-Driven Quality Management) for any CNC machine, regardless of the manufacturer. Relevant process and performance information from the CNC machine is uploaded in the form of servo traces and managed and analyzed via a simple browser application.

This makes it possible to gain insights into cause-and-effect relationships for individual machines or the entire production process. Control and regulation deviations, contour deviations, the currents of individual machine axes, and other performance indicators contained in the time-series data are made visible and usable. High-frequency recording of machine movements and control information provides insights into the machine's individual performance spectrum—a unique machine fingerprint. These signals can be analyzed, archived evaluated for tolerance, and compared using Smart Tracing.

With Aiktec–Digital Solutions, Klingelnberg addresses manufacturing companies seeking to make their production more transparent, efficient and future-proof. The digital solutions are specifically designed for industrial use and can be integrated into existing machine fleets, regardless of manufacturer or industry.

klingelnberg.com

ECM USA

STRENGTHENS SALES TEAM WITH MARCO MÖSER AS SENIOR SALES ENGINEER

ECM USA appointed Marco Möser to senior sales engineer for the western U.S.

Marco Möser

With more than 25 years of experience in the heat treatment industry, Möser brings extensive expertise in supporting OEMs on large-scale automotive programs.

Prior to joining ECM USA, he held senior leadership roles, including sales director and vice president, for specialized alloy fixturing and foundry organizations across Europe and the Americas. Throughout his career, he has demonstrated a consistent ability to drive sales growth, optimize performance, and strengthen team collaboration.

His professional background includes multiple executive-level positions, as well as completion of an Executive Development Program at The Wharton School in Philadelphia, further underscoring his leadership capabilities and strategic insight.

ecm-usa.com

Ceratizit

PROMOTES KUHNLE TO BUSINESS DEVELOPMENT SPECIALIST FOR DEFENSE

Ceratizit USA announced the promotion of Steve Kuhnle to U.S. business development specialist for Defense. Kuhnle previously served as the cutting tool company's sales director for the east region.

Steve Kuhnle

Kuhnle will focus on strengthening the company's engagement with the U.S. security and defense sector by identifying opportunities where the company's materials expertise and cutting tool technologies can best support manufacturers.

"Steve has been a valued member of our team for more than a decade and an ideal choice for this position," Managing Director Troy Wilt said.

"The combination of his institutional knowledge of Ceratizit, cutting tool solutions and the defense industry will be an asset to our customers in the U.S."

In addition, Kuhnle will immerse himself with customers to better understand their machining challenges and requirements while helping develop a portfolio of cutting tools and solutions tailored to the unique demands of security and defense applications.

"After more than 40 years in the cutting tool industry, I'm motivated to apply my experience to supporting defense manufacturers," Kuhnle said. "I look forward to helping them address manufacturing challenges with machining strategies and tooling technologies that improve efficiency and keep production moving."

ceratizit.com

Southern Gear

INVESTS IN ADVANCED MULTI-AXIS MACHINING PLATFORM

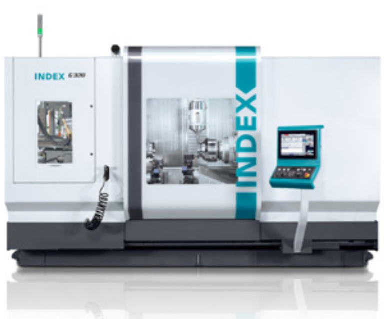

Southern Gear will install an advanced Index G320 Turn-Mill Center to produce medium-sized aerospace gears with high complexity and precision on a single machine.

By performing multiple operations, including turning, milling, spline and gear cutting, OD/ID grinding, and even power skiving on just one machine, Southern Gear expects to significantly reduce cost and lead times. The consolidation of processes will eliminate multiple setups and non-productive time, while ensuring exceptional bore-to-tooth, spline-to-tooth, and other critical concentricity and geometric accuracies.

The modular design of the Index G320 offers a wide range of machining capabilities and configurations. The system includes advanced multi-axis functionality, integrated tooling systems and turnkey process development to support complex part production. The machine features main and counter spindles designed for bar diameters up to 102 mm and chuck part diameters up to 315 mm.

Up to three tool carriers, with storage capacity for as many as 141 tools, can be integrated into the work area, providing maximum flexibility for complete machining of complex workpieces. The spacious work area accommodates shaft-type parts up to 1,400 mm in length.

The Index G320 includes a high-performance motor-milling spindle capable of simultaneous five-axis machining, supporting advanced processes such as spiral-bevel gear manufacturing through five-axis interpolation. Its rigid, vibration-damping mineral-cast mono-block machine bed, combined with large-dimension linear guides and rapid traverse rates up to 50 m/min, delivers exceptional speed, stability and productivity.

"The Index G320 is tailor-made for the high-precision, mid- to higher-volume gear projects we specialize in," Southern Gear National Sales Director Jim Granitsas said. "Bringing this level of capability into a single platform adds much-needed capacity and helps us shorten delivery timelines for an aerospace and defense supply chain that continues to face significant demand pressures. We're excited to begin quoting new opportunities where cost efficiency and lead time are critical."

southerngear.com

Griffin Gear

ACQUIRES BIRMINGHAM GEAR AND MACHINE

Griffin Gear, a portfolio company of Mangrove Equity Partners, announced the acquisition of Birmingham Gear and Machine. This strategic partnership strengthens Griffin Gear's market position by integrating a business that has highly complementary service offerings, customer base, and geographical reach.

It was founded in 1950 by Oscar Noles as Noles Machine and Welding, Birmingham Gear and Machine Co. The company evolved under the leadership of Noles' son, Royce, and eventually his grandsons Ock, Len and Royce Chambers who transitioned the business into a specialized gear and machine shop in 1989. In 2000, to support its continued growth, the company relocated to its current facility in Dora, AL.

Griffin Gear is proud to carry forward this multi-generational legacy. By leveraging the synergies between the two organizations, Griffin Gear aims to drive sustainable growth, operational efficiency and a continued commitment to exceptional customer service.

griffingear.com

Ryan Purcell

JOINS VECTOR COMPANIES AS MIDWEST REGIONAL SALES EXECUTIVE

Vector Cos. welcomed Ryan Purcell as Midwest regional sales executive, bringing more than two decades of industry and sales experience to the team.

Ryan Purcell

Since joining in January, Purcell completed an eight-week training program, working alongside team members across The Adams Co., Atlas Gear Co. Atlas Global and Northend Gear and Machine. The program gave him a hands-on understanding of products, processes, and how the company supports customers with reliable gearbox components and machining solutions.

A Midwest native, he is based out of the world headquarters and will support customers across Iowa, Illinois, Wisconsin, Missouri, Minnesota, North Dakota, and South Dakota.

theadamscompany.com

JUNE 25–29

WorldPM2026

The Metal Powder Industries Federation (MPIF) presents the largest global powder metallurgy (PM) and particulate materials event that only happens once every six years in North America. The PM industry will come together where three conferences, the WorldPM2026, AMPM2026 and Tungsten2026, will be sintered into one global event. (Montreal). The largest annual North American exhibit will showcase leading suppliers of metal powders, particulate materials, and metal additive manufacturing (AM)/3D printing process equipment, powders and products.

geartechnology.com/events/worldpm2026

JUNE 30–JULY 1

Dritev 2026

The automotive congress Dritev (DRIvetrain Transmission Electrification Vehicles) offers the powertrain community an optimal platform for exchange. Every year, decision-makers, experts and industry leaders from around the world meet in Baden-Baden, Germany. Here, vehicle manufacturers and suppliers exchange ideas and early capture innovations, developments and challenges in drive technology. During the two-day congress, experts from OEMs, suppliers, and universities present practical lectures on new trends as well as classical topics in drive technology.

geartechnology.com/events/dritev-2026

JULY 15–16

WZL Gear Conference USA

The WZL Gear Conference USA will take place on July 15 and 16, 2026, at Klingelnberg America, Inc. (Saline, MI). This renowned conference brings together North American companies with the Laboratory for Machine Tools and Production Engineering (WZL) at RWTH Aachen University and offers a compact overview of current developments and research topics in gear technology. Participating companies will have the opportunity to network with leading experts, discuss trends, and gain concrete insights to apply in their daily work.

geartechnology.com/events/wzl-gear-conference-usa-2026-03-26

SEPTEMBER 14–19

IMTS 2026

The largest manufacturing technology trade show in the Western Hemisphere (Chicago) and among the largest in the world, IMTS attracts nearly 90,000-130,000 attendees from over 112 countries. Pavilions include Gear Generation, Additive Manufacturing, Machine Components, Metal Cutting & Machining Centers, Tooling & Workholding Systems, Controls & CAD-CAM and Quality Assurance. From quality and inspection to process optimization, downtime reduction, cybersecurity, ergonomics, safety, and demand forecasting, the Industrial AI Arena showcases breakthrough tools, prototypes, and platforms – real solutions that redefine what's possible on the manufacturing floor.

geartechnology.com/events/imts-2026

AD INDEX

gear TECHNOLOGY®

FREE SUBSCRIPTION

24GTALL

☐ Renew my subscription ☐ NEW subscriber

☐ **YES** I want to receive/continue to receive ***Gear Technology*** ☐ **NO**

Name ______________________________

Job Title ______________________________

Company Name ______________________________

Company Address ______________________________

City ______________________________

State ______________________________

Zip Code ______________________________

Signature: ______________________________ *(required)*

Date: ______________

Please send

☐ PRINT Version

☐ DIGITAL Version (E-mail required)

E-MAIL: ______________________________

☐ BOTH Print and Digital

*You can OPT OUT at any time.

How are you involved with Gears?

(Check all that apply)

☐ My company **MAKES** gears

☐ My company **BUYS** gears

☐ I **DESIGN** gears

☐ I am a **SUPPLIER** to the gear industry

☐ Other (please describe)

____

What is your company's principal product or service?

____

Your mailing label on the cover looks like this:

X/Y - means you have recieved a complimentary copy. Please complete this form to continue receiving your FREE copy of *Gear Technology*.

Q14 (shown above) - means you have 14 issues remaining in your subscription (a NEW subscription has 16 issues).

Q1 - means you have 1 remaining issue before your *Gear Technology* subscription expires. Please complete this form to renew.

MAIL to: 1001 N. Fairfax St, Suite 500, Alexandria, VA 22314 USA | SCAN to: *subscribe@geartechnology.com* | FAX to: 1.847.437.6618

Tangencies

Aaron Fagan, Senior Editor

In the third century BCE, the Greek geometer Apollonius of Perga asked: How many circles can be drawn to touch three given circles, each at exactly one point? He answered it in his treatise *Tangencies,* concluding there are exactly eight distinct solutions to a single geometric constraint. The original text was lost, though a fourth-century report by Pappus of Alexandria preserved the result. When François Viète reconstructed the proof in the 1590s, the answer held. The problem endured not because it was abstract, but because it showed how much order hides inside a simple arrangement of curves.

That puzzle might feel remote from the shop floor. But its core question, how many solutions satisfy a set of geometric constraints, is one that gear engineers answer routinely. Every tooth contact analysis is, at bottom, a problem of the same kind: given curved surfaces and boundary conditions, how many valid configurations exist?

Consider a pair of gears in mesh. Under ideal conditions, the line of action, itself tangent to both base circles, produces a rolling point of contact that sweeps predictably along the involute profile. Tolerances, misalignment, tooth modifications, and load deflection complicate things. The questions that follow are practical but structurally familiar: How many actual engagement points exist across the face width? How evenly do they share load? How sensitive are those answers to the parameters we control?

Modern tooth contact analysis (TCA) software lets engineers simulate these scenarios in detail. Take a double-helical gear pair with a slight lead error on one helix. The software reveals what the shop floor eventually confirms: mesh crowds to one end of the face width, the load splits unevenly, and the gear set runs louder than predicted. Adjust the lead crown by just a few microns and the footprint re-centers, the load balances, and the noise drops. One constraint, slightly changed, rearranges the entire result. That is exactly the kind of sensitivity Apollonius would have recognized. The geometry has not changed in kind, only in degree, yet the practical outcome is transformed.

***The frontispiece engraving by Michael Burghers from Edmond Halley's 1710 edition of Apollonius'* Conics *depicts Aristippus, shipwrecked on Rhodes, spotting geometric figures drawn in the sand and telling his companions, "Raise your hopes, for I see the vestiges of mankind."* (Image: The Linda Hall Library.)**

Classical geometry reinforces the point. Depending on arrangement, two circles may share four common tangent lines, three, two, one, or none at all. Similarly, a slight deviation in a gear's helix angle, profile shift, or center distance can reduce a robust bearing pattern to a single line or open areas of no engagement entirely. Knowing where those thresholds fall, where a working solution tips into failure, is essential for reliability, noise reduction, and wear control. It is also what separates a gear that functions from one that performs.

Even the underlying mathematics rhymes. In Apollonius' problem, quadratic equations sort solutions by whether a tangent circle wraps around a given circle externally or nests inside it: positive and negative cases from one formula. In gear engineering, curvature plays a parallel role. Where a convex tooth flank meets a convex mating surface, engagement is fleeting and sensitive to error. Where convex meets concave, as in an internal gear mesh, contact wraps and stabilizes. The distributions on a simulated TCA map are real signatures of that interplay between positive and negative curvature, now expressed in steel rather than ink.

Pure geometry and practical gear design depend on counting, stability, and curvature. Apollonius enumerated tangent circles with a compass and straightedge, and we enumerate contact lines and load paths with finite element models and TCA software. Geometry is our inheritance, and while the tools we use to understand it have changed, the conversation with the past continues.

LeCount
Mandrel Selector

The Fastest Way to Your Expanding Mandrel

Choose the original LeCount® mandrel for any bore-clamping application. Each mandrel covers a defined range of bore sizes, providing versatility and precision for a wide variety of workpieces.

Whether you need a new, high-precision mandrel or re-certification of an existing one, Gleason ensures a fast and reliable process. With the material number of your current mandrel, Gleason can quickly identify the matching product.

www.gleason.com/lecount-selector

Total Gear Solutions **Gleason**